



## Research

**Cite this article:** Kuijpers MCM, Quigley CV, Bray NC, Ding W, White JD, Jackrel SL. 2025 Intraspecific divergence within *Microcystis aeruginosa* mediates the dynamics of freshwater harmful algal blooms under climate warming scenarios. *Proc. R. Soc. B* **292**: 20242520. <https://doi.org/10.1098/rspb.2024.2520>

Received: 19 October 2024

Accepted: 3 January 2025

**Subject Category:**

Ecology

**Subject Areas:**

ecology, genetics, microbiology

**Keywords:**

intraspecific diversity, climate warming, cyanobacterial harmful algal blooms, local adaptation, heat shock protein gene expression

**Author for correspondence:**

Sara L. Jackrel

e-mail: [sjackrel@ucsd.edu](mailto:sjackrel@ucsd.edu)

Electronic supplementary material is available online at.

# Intraspecific divergence within *Microcystis aeruginosa* mediates the dynamics of freshwater harmful algal blooms under climate warming scenarios

Mirte C. M. Kuijpers<sup>1</sup>, Catherine V. Quigley<sup>2</sup>, Nicole C. Bray<sup>2</sup>, Wenbo Ding<sup>1</sup>, Jeffrey D. White<sup>2</sup> and Sara L. Jackrel<sup>1</sup>

<sup>1</sup>Department of Ecology, Behavior and Evolution, School of Biological Sciences, University of California San Diego, La Jolla, CA, USA

<sup>2</sup>Department of Biology, Framingham State University, Framingham, MA, USA

MCMK, 0000-0002-5409-2129; WD, 0009-0000-0853-6123; JDW, 0000-0002-0805-5706; SLJ, 0000-0001-7326-4996

Intraspecific biodiversity can have ecosystem-level consequences and may affect the accuracy of ecological forecasting. For example, rare genetic variants may have traits that prove beneficial under future environmental conditions. The cyanobacterium responsible for most freshwater harmful algal blooms worldwide, *Microcystis aeruginosa*, occurs in at least three types. While the dominant type occurs in eutrophic environments and is adapted to thrive in nutrient-rich conditions, two additional types have recently been discovered that inhabit oligotrophic and eutrophic environments and have genomic adaptations for survival under nutrient limitation. Here, we show that these oligotrophic types are widespread throughout the Eastern USA. By pairing an experimental warming study with gene expression analyses, we found that the eutrophic type may be most susceptible to climate warming. In comparison, oligotrophic types maintained their growth better and persisted longer under warming. As a mechanistic explanation for these patterns, we found that oligotrophic types responded to warming by widespread elevated expression of heat shock protein genes. Reduction of nutrient loading has been a historically effective mitigation strategy for controlling harmful algal blooms. Our results suggest that climate warming may benefit oligotrophic types of *M. aeruginosa*, potentially reducing the effectiveness of such mitigation efforts. In-depth study of intraspecific variation may therefore improve forecasting for understanding future whole ecosystem dynamics.

## 1. Introduction

Variation within a species can rival the effects of variation among species in regulating whole ecosystem dynamics, including biogeochemical cycling [1,2]. Standing genetic variation within a species can also be a critical resource when leveraged in response to changing environmental conditions. Using a species that is known to have widespread ecosystem level effects under current environmental conditions, we investigate how standing intraspecific variation may elucidate future ecosystem-level impacts of a species under climate warming.

Cyanobacteria (formerly blue-green algae) are a clade of photosynthetic prokaryotes and the oldest known oxygen-producing organisms on Earth, with fossils dating back to before the great oxidation event [3]. The clade is found across a diversity of environments, including eutrophic and

oligotrophic lakes and tropical and polar regions [4,5]. Many species can form dense, and sometimes toxic, blooms which visibly discolour their freshwater, brackish or marine environment and often have negative impacts on their ecosystem [6]. These blooms also incur significant costs to tourism, agriculture, and human health [7].

The cyanobacterial clade has survived major changes in the Earth's climate and bloom-forming species now seem to be benefiting from the effects of anthropogenic climate change [6,8]. This includes more extreme precipitation (which can lead to increased nutrient run-off into aquatic systems), droughts (which can lead to increased retention time of cyanobacteria within lakes) and, critically, increased temperatures (which often give cyanobacterial species a competitive advantage over eukaryotic algae) [8]. The advantages of higher temperatures to bloom-forming cyanobacteria are twofold. First, higher temperatures lead to increased stratification of warmer water which favours buoyant cyanobacterial species while causing increased sedimentation of non-buoyant eukaryotic algal species [9]. Second, many cyanobacteria have a competitive growth advantage at higher temperatures, with optimal growth rates for cyanobacterial species often above 25°C [10,11]. Cyanobacterial blooms may even create a positive feedback loop in which warmer waters promote blooms, which, due to highly concentrated photo-absorption within the dense cyanobacterial blooms, leads to further warming of the surface waters [12,13]. A better understanding of the interaction of harmful bloom-forming cyanobacteria and climate warming will therefore be important for the prediction and mitigation of such harmful blooms in the future.

*Microcystis aeruginosa* is a widely distributed cyanobacterium that produces the hepatotoxin microcystin [14]. Toxic blooms of *M. aeruginosa* have caused mass wildlife mortality events and have threatened human drinking water supplies [14–17]. *Microcystis aeruginosa* was previously found to exist as at least three distinct genotype–environment groups (hereafter 'bacterial types') across lakes spanning a wide range of phosphorus levels in MI, USA [5]. The first bacterial type, which we refer to as high-nutrient lake/high-nutrient genotype or HL/HG, encompasses strains found in nutrient-rich conditions and contains the most well-known type of *M. aeruginosa* identified in eutrophic systems throughout the world. There is extensive genotypic diversity within this type, which has been well described previously [5]. A second bacterial type, which we refer to as LL/LG (low-nutrient lake/low-nutrient genotype), is restricted to oligotrophic, nutrient-poor ecosystems while the third bacterial type, which we refer to as HL/LG (high-nutrient lake/low-nutrient genotype), is most phylogenetically related to LL/LG but in fact occurs in eutrophic and mesotrophic lakes. The HG versus LG classifications were originally determined using metagenome similarity-based clustering, with the genomes in the LG cluster showing signs of genome streamlining [5]. The HL classification is assigned to strains isolated from eutrophic and mesotrophic lakes, whereas the LL classification is assigned to strains isolated from oligotrophic lakes using a 10 µg l<sup>-1</sup> total phosphorus (TP) threshold for the oligotrophic–mesotrophic boundary [18]. Overall, this classification of *M. aeruginosa* strains into these three types is well supported by (i) a highly resolved multi-gene phylogeny, (ii) clustering of genome characteristics (particularly enrichment of genome streamlining traits in the oligotrophic types) and (iii) strong similarity within types in functional capability, as determined by a genome-wide protein functional analysis using shotgun metagenomics [5]. Our prior work suggests that the HL/LG bacterial type takes advantage of low-nutrient microenvironments within eutrophic and mesotrophic lakes, as both LL/LG and HL/LG strains show adaptations that would facilitate survival in low-nutrient conditions [5].

Harmful blooms of *M. aeruginosa* are thought to be primarily driven by excess nutrient loading, with reduction in phosphorus run-off into freshwater systems often proving successful in bloom reduction [19]. Populations of *M. aeruginosa* can experience stress from both N and P limitation, particularly during established late-stage phases of blooms [16]. Therefore, oligotrophic types may be situated to thrive within the later stages of blooms. Concerningly, *M. aeruginosa* appears not only to have a competitive growth advantage but also to produce more toxins at higher temperatures [8]. Harmful blooms of *M. aeruginosa* may therefore become more frequent and severe with climate change, and indeed, this may already be occurring in one of the largest lakes in China, Lake Taihu [17].

While *M. aeruginosa* has a growth advantage at higher temperatures, increased temperatures are a cellular stressor that will become detrimental to *M. aeruginosa* above a certain threshold. Specifically, increased temperatures can promote the misfolding of newly synthesized proteins, as well as denaturation and damage to existing proteins [20]. The heat shock proteins (HSPs) are a highly conserved and ubiquitous family of molecular chaperones, which can increase stress tolerance by preventing protein misfolding and preserving protein homeostasis under stress [21]. While constitutive HSPs are expressed at low levels under normal conditions, the expression of inducible forms of HSPs is greatly increased at elevated temperatures [22]. Thermotolerance is characterized by elevated expression of inducible forms of HSPs [23]. Not only does *M. aeruginosa* have higher optimal temperatures than many eukaryotic algae, but the cyanobacterium may also show increased tolerance to higher temperatures due to frequent exposure to elevated temperatures caused by photon-absorption of dense blooms near the lake surface [13]. We, therefore, hypothesize that certain types of *M. aeruginosa*, such as those occurring in late-stage blooms, might show elevated expression of HSPs as a means for withstanding elevated temperatures.

Understanding the effects of warming on different types of *M. aeruginosa* will be essential to predict the frequency, duration and intensity of harmful blooms under climate warming. Here, we isolated strains of *M. aeruginosa* from lakes of varying trophic status across the midwestern and northeastern USA. We found that oligotrophic types previously identified in a small region of Michigan are widespread throughout a much broader geographic region, expanding the relevance of these oligotrophic types for harmful algal blooms [5]. We then employed strains from each of the three types of *M. aeruginosa* in an experimental warming study, using four temperatures ranging from 20°C to 32°C, with the aim of evaluating the growth responses of strains belonging to each type under elevated temperatures. Next, we investigated the mechanisms of thermotolerance within each type by analysing the expression of HSPs during the warming study. Additionally, we evaluated the expression of one of the genes in the microcystin (*mcy*) operon, which is responsible for production of the hepatotoxin microcystin. Overall, our results clarify the current and potentially future relevance of oligotrophic types of *M. aeruginosa*, contributing to our ability to predict and manage harmful algal blooms under climate warming.

## 2. Methods

### (a) Isolation and culturing of *M. aeruginosa*

Sampling and isolation methods are fully described elsewhere [5,24]. In brief, we collected *M. aeruginosa* and water samples for nutrient analysis (electronic supplementary material, table S1) from lakes spanning a large productivity gradient (5.8–65  $\mu\text{g l}^{-1}$  TP) in the midwestern and northeastern USA from July to August 2019. *Microcystis* colonies were isolated from water samples via sequential pipette transfers using sterile 0.5 $\times$  WC-S medium and a dissecting microscope [25]. These ‘washed’ colonies were inoculated into 20 ml volumes of media. Only colonies with a distinctive shape and compact cell arrangement were selected rather than loose aggregations of cells. Successfully established isolates were maintained at 21°C in 200 ml cultures under a 12:12 h light:dark cycle with 80  $\mu\text{mol m}^{-2} \text{s}^{-1}$  fluorescent lighting. Inoculums of each culture were transferred monthly to fresh media. While these cultures are not axenic, only closely associated bacteria should have remained after the initial isolation procedure [26]. See methodology for strain genotyping and phylogenetics analyses in the electronic supplementary material.

### (b) Warming experiment

We acclimated one biological replicate of each of 20 of our 24 isolated *M. aeruginosa* strains (electronic supplementary material, table S1) to four temperatures, 20°C, 24°C, 28°C and 32°C, by gradually adjusting the temperature over 48 h. We chose a single biological replicate per strain to focus our experimental design on bacterial types. We consider each strain as an independent replicate of the same bacterial type, supported by previous work showing strong genomic similarities between strains of the same type. Four deionized water baths were set up within a refrigerated incubator (Percival) with an ambient internal chamber of 20°C. Heated treatments were warmed to their desired targets and maintained by submersible heaters. Each acclimated strain  $\times$  temperature combination was inoculated into 125 ml flasks of 0.5 $\times$  WC-S medium and immersed in their respective bath. To minimize variation in initial cell densities across treatments, we targeted an *M. aeruginosa* biomass equivalent to 1  $\mu\text{g l}^{-1}$  chlorophyll-*a*, which is a routinely used surrogate for phytoplankton biomass. Cultures were grown without media replacement under a 12:12 h light:dark cycle throughout the experiment. Biomass was subsampled weekly for the duration of the 35 day experiment by vacuum-filtering 10 ml aliquots per flask onto 23 mm A/E glass fibre filters (Pall). Filters were immediately frozen until used to determine *M. aeruginosa* growth via fluorometric analysis of chlorophyll-*a* following a 24 h dark extraction in cold 90% ethanol, with acidification (Turner Designs) [24]. On day 35, a second replicate filter was collected and stored long term at –80°C until RNA extraction.

### (c) Quantifying gene expression

We extracted RNA with Invitrogen *mirVana* miRNA Isolation Kits following the protocol modifications of Fortunato & Huber [27]. We synthesized cDNA using the SuperScript III First-Strand Synthesis System and random hexamer primers. Quantitative real-time PCR was then performed for *M. aeruginosa* gene targets that are involved in heat stress responses (ClpB, DnaJ, DnaK1, DnaK3, DnaK-fp, GroEL, GroES, GrpE, HrcA, Hsp20, HspA, HtpG) and the reference housekeeping gene *rpoA*, using custom primers designed for *M. aeruginosa* [28]; as well as the gene *mcyE* that correlates with toxin production using HEP primers [29–31]. See methods in electronic supplementary material for details of gene expression analysis and all statistical analyses.

## 3. Results

We found LL/LG and HL/LG types previously described from oligotrophic lakes within an 8550 km<sup>2</sup> region in Michigan span a wider geographic range across the midwest and northeastern USA (figure 1; electronic supplementary material, figure S2). We then used 20 strains in a warming experiment, including seven assigned to HL/HG, five to HL/LG and seven to LL/LG. The final strain, belonging to a bacterial type not found in our prior work as it had an HG genotype but originated from an oligotrophic lake, was excluded from further analyses.

We first evaluated *M. aeruginosa* growth patterns during exponential growth in Week 1 of the warming study. We found that exponential growth varied by bacterial type, with a trend of type-specific responses to temperature (figure 2; linear mixed-effects (LME) model: type  $F_{2,16} = 164.16$ ,  $p = 0.035$ ,  $\eta^2p = 0.34$ ; temperature  $F_{3,48} = 2.55$ ,  $p = 0.067$ ,  $\eta^2p = 0.14$ ; type  $\times$  temperature  $F_{6,48} = 2.070$ ,  $p = 0.074$ ,  $\eta^2p = 0.21$ ). Similarly, we found strong support for different responses to temperature by each type when using a hierarchical general additive model (GAM) framework, which does not have an assumption of linearity (electronic supplementary material, table S2, GAM: type-specific trendlines  $p = 0.001$ ,  $R^2 = 27.9\%$ ). We found that most strains grew with similar or higher growth rates at 24°C compared with 20°C: only two of seven HL/HG strains (28.6%), zero of five HL/LG strains (0%) and one of seven LL/LG (14.3%) had lower growth rates at 24°C than 20°C with median increases in growth rate from 20°C to 24°C for persisting strains of +78.2, +20.8 and +16.3%, respectively. In contrast, at higher temperatures, LG strains were less negatively affected by temperature than HL/HG strains, specifically, six of seven HL/HG strains (85.7%) had lower growth rates for 28°C compared with 20°C, while HL/LG had two of five (40%) and LL/LG had three of seven (42.9%) with median differences in growth rate from 20°C to 28°C for persisting strains of –15.0, +10.4 and +1.4%, respectively. At the highest temperature, all bacterial types had several strains negatively affected by temperature, as four of seven HL/HG (57.1%), two of five HL/LG (40%) and four of seven LL/LG strains (57.1%) showed lower growth rates at 32°C when compared

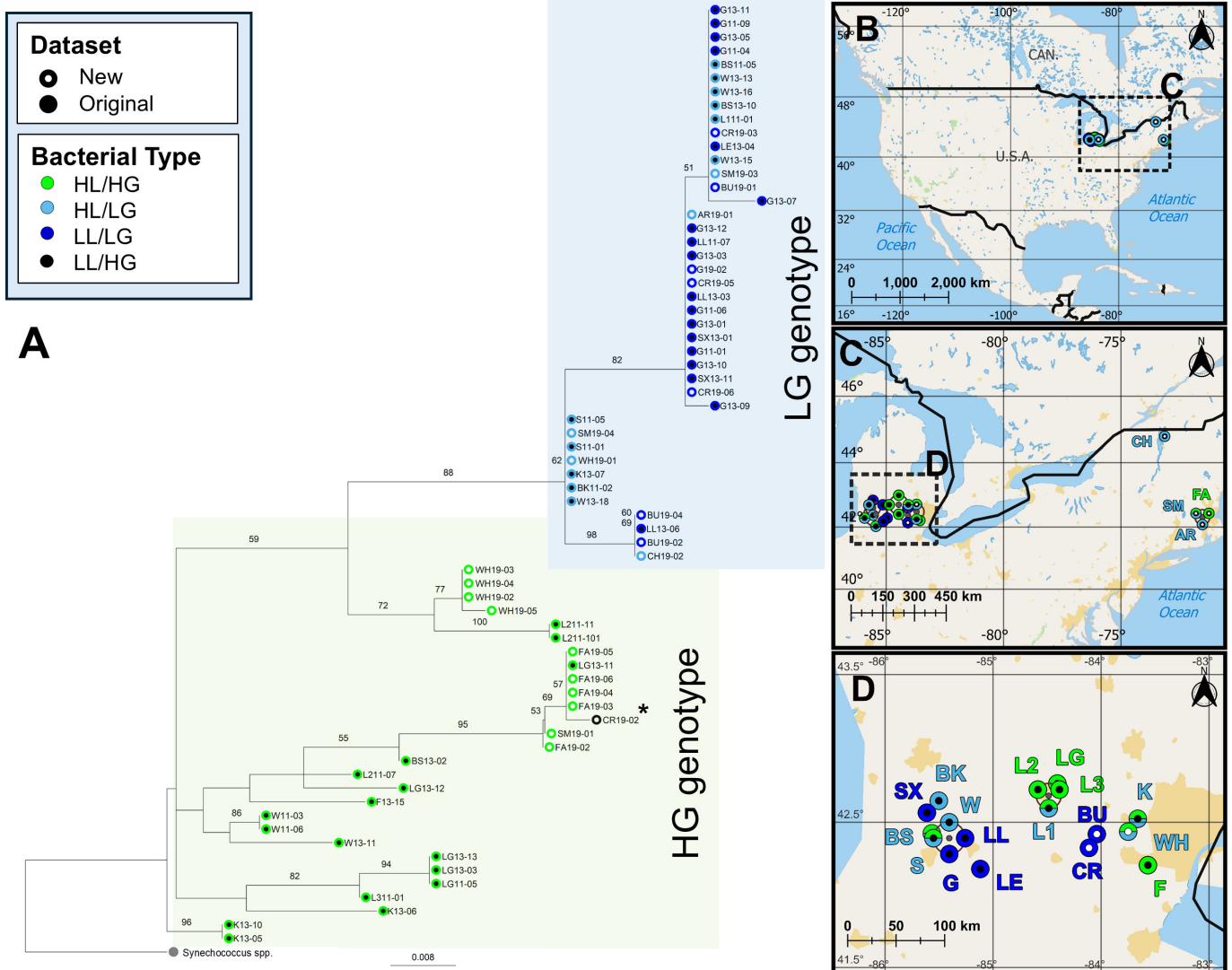


**Figure 1.** (A) Phylogenetic placement of 24 strains of *Microcystis aeruginosa* isolated in 2019 from lakes in the midwest and northeastern USA. These strains are nested within a larger phylogeny from our original dataset, isolated in 2011–2013 from an 8550 km<sup>2</sup> region of MI, USA. Phylogeny based on the rRNA-ITSc region obtained via Sanger sequencing for 2019 strains and via extraction from metagenome assembled genomes for 2011–2013 strains. F19–02, G19–01 and CR19–01 excluded from phylogeny due to poor sequence quality. Placement of CR19–01, when included despite quality, indicated by asterisk. (B–D) Geographic origin of all strains. Filled dots indicate *M. aeruginosa* bacterial type, as determined by multi-locus sequence typing of metagenome-assembled genomes as described in [5]. Open dots indicate assigned bacterial type for 2019 isolates. Dark blue rings depict *M. aeruginosa* originating from oligotrophic lakes (LL/LG); light-blue depicts those from eutrophic and mesotrophic lakes that phylogenetically cluster with oligotrophic lakes (HL/LG type); green depicts all others from eutrophic and mesotrophic lakes (HL/HG); and half light-blue, half green rings (shown in maps) depict lakes where both HL/LG and HL/HG were isolated. See electronic supplementary material, table S1 for strain and lake metadata. HL, high-nutrient lake; HG, high-nutrient genotype; LG, low-nutrient genotype; LL, low-nutrient lake.

with 20°C, but overall LG strains were less negatively affected with a median difference in growth rate from 20°C to 32°C for persisting strains of HL/LG at +137%, LL/LG at +26.1% and HL/HG at -20.4%.

Upon evaluating growth patterns across the entire four week study, we find that growth was again context dependent on bacterial type (figure 3; electronic supplementary material, figure S3; LME with week as random effect: type  $F_{2,70} = 5.03$ ,  $p = 0.009$ ,  $\eta^2 p = 0.13$ ; temperature  $F_{3,219} = 2.79$ ,  $p = 0.042$ ,  $\eta^2 p = 0.04$ ; type  $\times$  temperature  $F_{6,219} = 1.26$ ,  $p = 0.28$ ; see electronic supplementary material, figure S3 for LME with week as fixed effect). Furthermore, we find strong support for type-specific responses to temperature when dropping assumptions of linearity (electronic supplementary material, table S2, GAM: type-specific trendlines  $p = 0.008$ ,  $R^2 = 23.7\%$ ; see electronic supplementary material, figure S3 for GAM with week as a fixed effect). In particular, HL/LG strains tended to be less negatively affected by higher temperatures. However, all three types show marked decline by Week 4, by which time inorganic nutrients may have become scarce. Specifically, HL/LG has the highest average growth rate across all temperatures and weeks (Tukey's tests: HL/HG versus HL/LG  $p = 0.008$ , HL/HG versus LL/LG  $p = 0.760$ , HL/LG versus LL/LG  $p = 0.046$ ). Additionally, while growth rates across the four weeks do not show significant differences between bacterial types for 20°C and 24°C, there is a trend of higher growth rates for HL/LG versus HL/HG strains at 28°C and 32°C, with HL/LG also differing from LL/LG at 32°C (Tukey's tests: 28°C HL/LG versus HL/HG  $p = 0.05$ ; 32°C HL/LG versus HL/HG  $p = 0.035$ , HL/LG versus LL/LG  $p = 0.006$ ; all other comparisons:  $p > 0.100$ ).

By Week 4, all bacterial types had multiple strains starting to decline across all temperatures, but LG strains showed overall greater persistence. Across all temperatures, we found positive growth rates in 6 of 28 HL/HG populations (21.4%), 10 of 20 HL/LG populations (50%), and 19 of 28 LL/LG populations (67.9%). We note that in Week 1, all HL/HG strains show positive

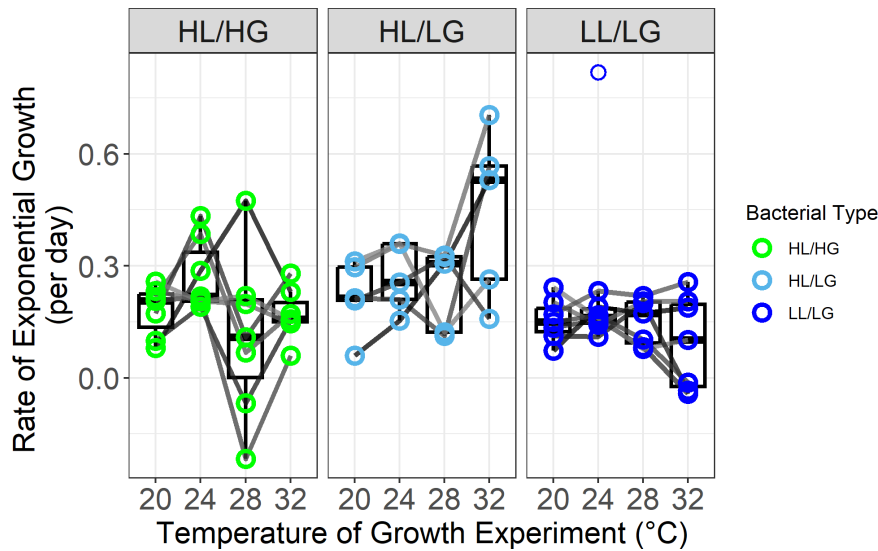


**Figure 2.** Exponential growth rates of oligotrophic types of *Microcystis aeruginosa*, HL/LG (5 strains) and LL/LG (7 strains), were, respectively, elevated or less negatively affected under warmer temperatures than the eutrophic HL/HG type (7 strains). Lines connect measurements of each strain grown across four temperatures. LME model showed a significant effect of type ( $p < 0.05$ ), and a weaker effect of temperature and their interaction ( $p < 0.08$ ). Further, a GAM with a type-specific responses to temperature fitted the data significantly better than a global response GAM. Note, the LL/LG outlier at 24°C is omitted from the strain's trendline but retained in statistical analysis. HL, high-nutrient lake; HG, high-nutrient genotype; LG, low-nutrient genotype; LL, low-nutrient lake.

growth, while three LL/LG strains show negative growth. However, we previously found that LL/LG strains generally grow more slowly, which coupled with low cell densities at the start of the experiment, may have been more prone to measurement errors that indicated negative growth while the more rapidly growing HL/HG strains show clear early growth followed by rapid decline in the following weeks.

Further, population persistence (defined as holding a positive growth rate) over the four week experiment showed a strong dependence on both temperature and bacterial type (figure 3; CLMM: type:  $p < 0.01$ , temperature:  $p < 0.01$ , type  $\times$  temperature:  $p = 0.45$ ). Specifically, population persistence of HL/HG was notably lower at warmer temperatures, whereas a higher percentage of populations of the oligotrophic types persisted through the end of the study. For example, by Week 3, only 37.5% (four of seven) of HL/HG populations growing at 32°C showed positive growth compared with 100% (seven of seven) of LL/LG populations. We see similar results when comparing LG versus HG genotypes at 28°C, with three HG strains (28.6%) showing negative growth rates at Week 2, five (71.4%) by Week 3 and all (100%) strains no longer persisting by Week 4, while only one LG strain (7.7%) is non-persisting by Week 2, three (23.1%) by Week 3 and only seven (53.8%) by Week 4.

Next, we ran separate models for each bacterial type. The HL/HG type showed an effect of temperature on growth rates averaged across the four week experiment (HL/HG: temperature:  $F_{3,81} = 4.28$ ,  $p = 0.007$ ,  $\eta^2 p = 0.14$ ). Specifically, we found that HL/HG growth at 28°C was slower than the growth at both 20°C and 24°C, while the growth rate at 32°C did not differ significantly from the other temperatures (Tukey's tests: 28°C versus 20°C  $p < 0.05$ , 28°C versus 24°C  $p < 0.05$ , all other comparisons  $p > 0.10$ ). In contrast, the two oligotrophic types were not affected by temperature (HL/LG: temperature:  $F_{3,57} = 0.626$ ,  $p = 0.601$ ,  $\eta^2 p = 0.03$ ; LL/LG: temperature:  $F_{3,81} = 1.55$ ,  $p = 0.208$ ,  $\eta^2 p = 0.05$ ).

Given that these results suggest that climate warming may have differing effects on oligotrophic versus eutrophic types of *M. aeruginosa*, we aimed to further understand this phenomenon by evaluating the genetic content and gene expression responses of each bacterial type under warming scenarios. Surveying shotgun metagenomic datasets of previously collected *M. aeruginosa*, we found strain-level variation in copy number for genes involved in regulating thermotolerance (electronic supplementary material, figure S4). To directly measure thermotolerance as a result of both differential gene copy number and expression, we first tested for a widespread response of HSP family gene targets by including all measured HSPs in a single model. Here, we found that the effects of temperature on gene expression were highly bacterial type-specific (figure 4; electronic supplementary material, figures S5 and S6; analysis of variance (ANOVA): type:  $F_{2,16} = 2.17$ ,  $p = 0.12$ ,  $\eta^2 p = 0.02$ ; temperature:  $F_{2,402} = 10.02$ ,  $p < 0.01$ ,  $\eta^2 p = 0.05$ ; type  $\times$  temperature:  $F_{4,402} = 3.67$ ,  $p < 0.01$ ,  $\eta^2 p = 0.04$ ); however, we note that a large percentage of the variance in gene expression was not explained by our model, as indicated by the effect sizes. Most notably, the LL/LG type, whose growth rates were largely unaffected by temperature, showed markedly elevated expression of HSPs at warmer temperatures in comparison to other bacterial types (figure 4; electronic supplementary materials, figure S6). LL/LG had the highest mean relative gene expression in 58.3% of all 36 gene-by-temperature combinations and, notably, the highest expression in 75% of all 12 combinations within the 32°C treatment (figure 4). Further, the HL/LG type most often exhibited intermediate expression between the other two types. This ordered pattern of expression (i.e. HL/HG  $<$  HL/LG  $<$  LL/LG) was evident at warmer temperatures, including 46% of all 24 gene-by-temperature combinations at 28°C and 32°C (figure 4).

Given that constitutive versus inducible forms of HSPs may respond differently to thermal stress, we next focused on each target gene individually. We found that HSP expression declined with temperature, as would be expected for constitutively expressed proteins, including chaperones, for six different HSP targets (electronic supplementary material, figure S5; ANOVAs with fixed effect of temperature for ClpB:  $F_{2,28} = 7.41$ ,  $p < 0.01$ ,  $\eta^2 p = 0.35$ ; DnaJ:  $F_{2,28} = 12.66$ ,  $p < 0.01$ ,  $\eta^2 p = 0.47$ ; DnaK-fp:  $F_{2,28} = 8.20$ ,  $p < 0.01$ ,  $\eta^2 p = 0.37$ ; DnaK3:  $F_{2,28} = 17.55$ ,  $p < 0.01$ ,  $\eta^2 p = 0.56$ ; HrcA:  $F_{2,28} = 8.23$ ,  $p < 0.01$ ,  $\eta^2 p = 0.37$ ; HtpG:  $F_{2,28}$

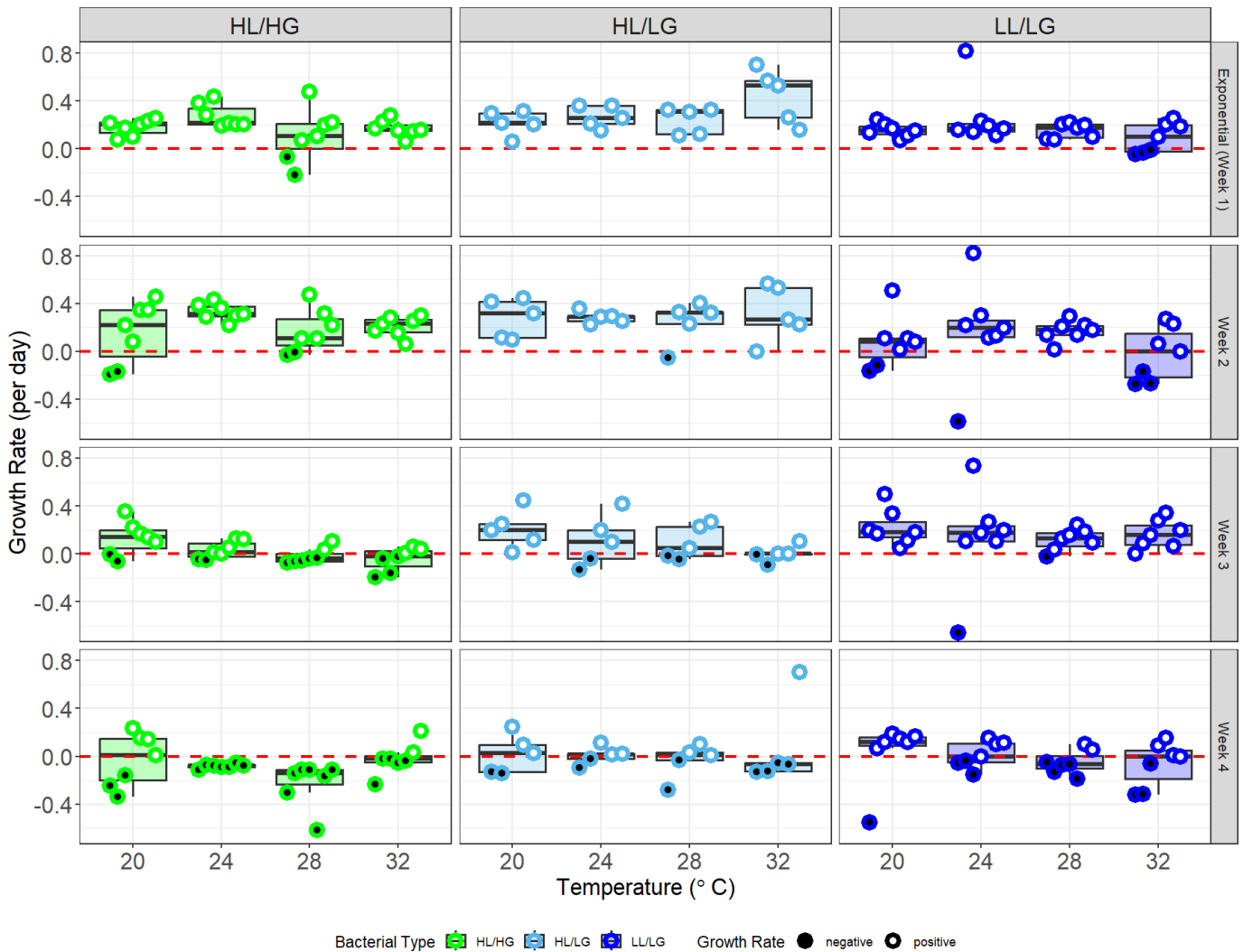


**Figure 3.** Bacterial type predicts growth rates and population persistence of *Microcystis aeruginosa* (see growth curves in electronic supplementary material, figure S3). Negative growth rates (i.e. population decline) shown with filled black data points and positive growth rates (i.e. population persistence) shown with open white points. Points spread on the x-axis for visibility but have no y-axis value alteration. LME model indicated significant effect of type ( $p < 0.01$ ) and temperature ( $p < 0.05$ ) on growth rates. A GAM with type-specific responses to temperature performed significantly better than a global response GAM. A cumulative link mixed-effect model for population persistence with strain and time point as random effects showed a significant effect of type and temperature. GAM, general additive model; HL, high-nutrient lake; HG, high-nutrient genotype; LG, low-nutrient genotype; LL, low-nutrient lake.

$= 3.47$ ,  $p = 0.045$ ,  $\eta^2 p = 0.20$ ). Toxin gene expression also declined with temperature for each bacterial type (electronic supplementary material, figure S7; *mcyE*:  $F_{2,28} = 12.09$ ,  $p < 0.01$ ,  $\eta^2 p = 0.46$ ). However, in sharp contrast to this decline in expression with temperature, two HSPs were upregulated among oligotrophic types at warmer temperatures (electronic supplementary material, figure S5; ANOVA type  $\times$  temperature for DnaK1:  $F_{4,28} = 2.83$ ,  $p = 0.044$ ,  $\eta^2 p = 0.29$  and Hsp20:  $F_{4,28} = 2.90$ ,  $p = 0.040$ ,  $\eta^2 p = 0.29$ ). Further, our results suggest a more finely tuned response to temperature increase in LG versus HG genotypes. Specifically, for LL/LG, five genes were differentially expressed between 24°C and 32°C (Tukey's tests: DnaJ, DnaK-fp, DnaK3, MycE, Hsp20 and HtpG, all  $p < 0.05$ ), and three were differentially expressed between 28°C and 32°C (MycE, DnaK1, and Hsp20, all  $p < 0.05$ ). Similarly, for HL/LG, three genes were differentially expressed between 24°C and 32°C (Tukey's tests: DnaJ, DnaK3, and HrcA, all  $p < 0.05$ ), and four were differentially expressed between 28°C and 32°C (DnaJ, DnaK-fp, DnaK3 and HrcA, all  $p < 0.05$ ). In contrast to these results for oligotrophic types, for HL/HG, we found less evidence of differential expression. Specifically, while four genes were differentially expressed between 24°C and 32°C (Tukey's tests: DnaJ, DnaK3, MycE and HrcA, all  $p < 0.05$ ), none were differentially expressed between 28°C and 32°C.

While we found clear variation between bacterial types, substantial variation within types in terms of both growth dynamics and gene expression is evident. We found that despite this intratype variation, bacterial type is a strong predictor of strain growth and expression rates (MANOVA: type  $F_{34,58} = 2.74$ ,  $p < 0.001$ ,  $\eta^2 p = 0.62$ ; temperature  $F_{34,58} = 1.39$ ,  $p = 0.131$ ; type  $\times$  temperature:  $F_{68,124} = 0.70$ ,  $p = 0.950$ ). Additionally, bacterial type remains a significant predictor when considering only growth dynamics or only gene expression rates in separate multivariate models (growth dynamics only model: type  $F_{8,84} = 2.24$ ,  $p = 0.032$ ,  $\eta^2 p = 0.18$ ; temperature  $F_{8,84} = 1.87$ ,  $p = 0.075$ ,  $\eta^2 p = 0.15$ ; type  $\times$  temperature:  $F_{16,176} = 0.89$ ,  $p = 0.584$ ; Gene expression only model: type  $F_{26,66} = 3.40$ ,  $p < 0.0001$ ,  $\eta^2 p = 0.57$ ; temperature  $F_{26,66} = 0.97$ ,  $p = 0.520$ ; type  $\times$  temperature:  $F_{52,140} = 0.58$ ,  $p = 0.99$ ). We also found clear clustering by type using a linear discriminates analysis. Specifically, LG and HG strains separated along the first axis of discrimination, which explained 74.7% of the between-class variation and was most heavily weighted by Week 3 and 4 growth rates, and ClpB, DnaK3, DnaK-fp, GroES, GroEL, Hep, HrcA, HspA, and Hsp20 expression; while HL/LG and LL/LG

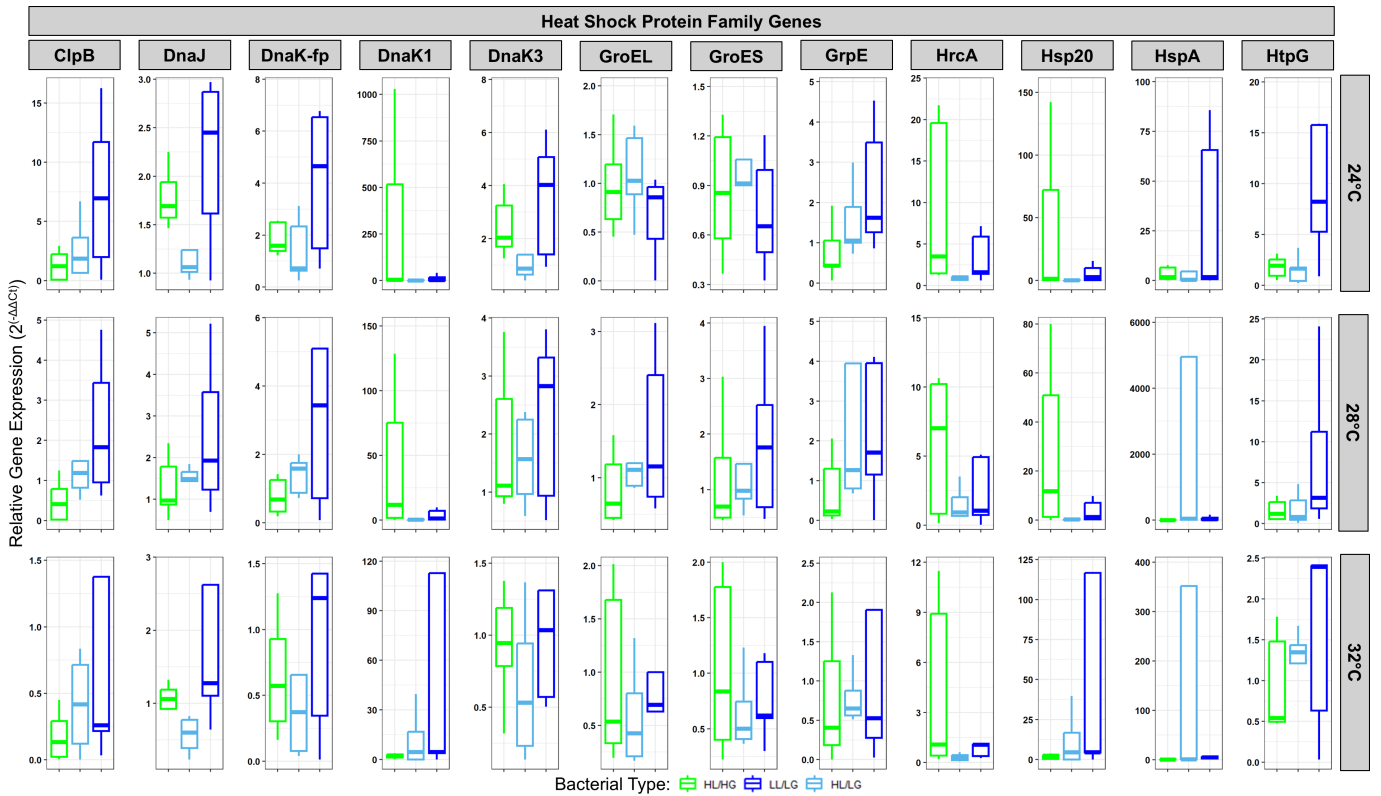


**Figure 4.** Bacterial type-specific responses to temperature of *Microcystis aeruginosa* through differential expression of genes encoding for heat shock. Type-specific responses to temperature were also observed for two models run on individual gene targets DnaK1 and Hsp20. Relative gene expression calculated as  $2^{-\Delta\Delta C_t}$ , with *rpoA* as the reference gene and 20°C as the reference condition. For visualization, each faceted plot has its own y-axis. See electronic supplementary material, figure S5 for the same data highlighting within-type responses to temperature and electronic supplementary material, figure S6 for normalized rather than raw data, with individual data points shown.

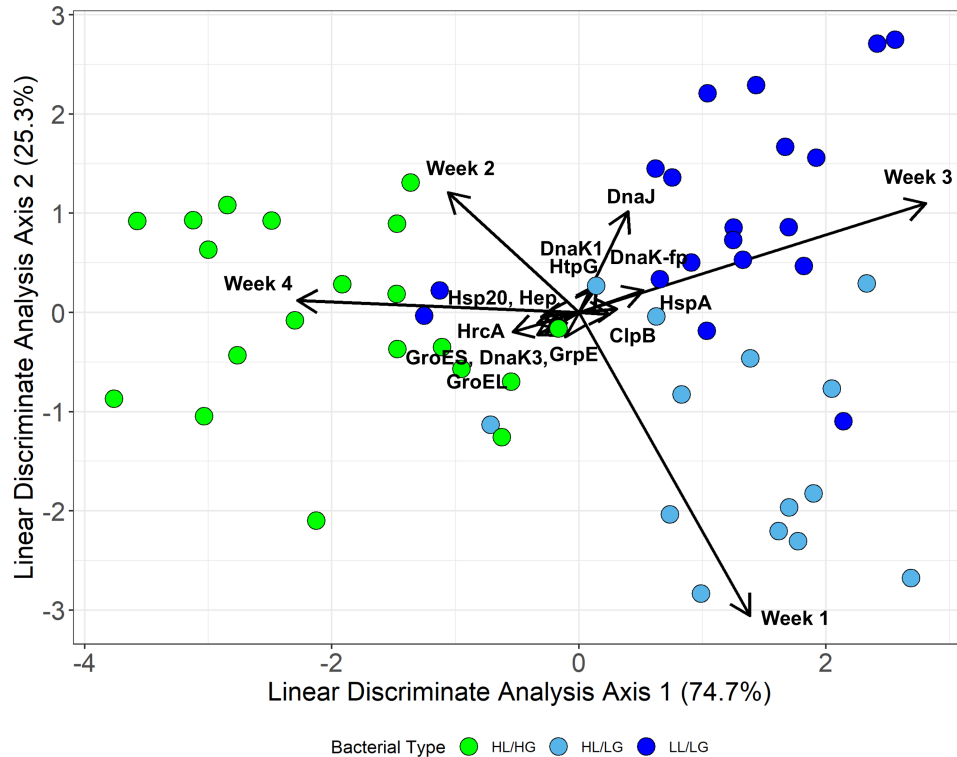


**Figure 5.** Bacterial types differ in overall patterns of growth and gene expression dynamics via linear discriminant analysis. Arrows indicate coefficients of variance explained by each variable (see electronic supplementary material, figure S8 for magnification of gene expression arrows). Data for all temperatures except 20°C are included in the model to allow for the calculation of relative gene expression with 20°C as the baseline. Week *x* refers to the growth rate during that week.

strains separated along the second axis of discrimination, which explained 25.3% of the between-class variation and was most heavily weighted by differences in week 1 and 2 growth rates, and DnaK1, DnaJ, GrpE, and HtpG expression rates (figure 5; electronic supplementary material, figure S8 and table S3).

## 4. Discussion

*Microcystis aeruginosa* is the dominant cause of freshwater harmful algal blooms worldwide and can inhabit an impressive range of environments that span over 20-fold in phosphorus levels due in part to extensive genetic diversity [32–34]. We show that this intraspecific biodiversity within *M. aeruginosa* is essential for predicting how this cyanobacterium will respond to the warming climate [6]. Overall, our results suggest that the *M. aeruginosa* types show different patterns of growth in response to temperature, both during exponential growth and across a month of heat exposure. We find that oligotrophic-adapted bacterial types of *M. aeruginosa* are more likely to survive long term at higher temperatures, with their exponential rates of growth generally unaffected by or even benefitting from much warmer temperatures. In contrast, the classic eutrophic type of *M. aeruginosa* showed a notable decrease in growth rate and population persistence at higher temperatures, especially across longer timespans, suggesting that climate warming may cause strains of this type to experience a competitive disadvantage. Interestingly, the typically slower growing LL/LG was generally intermediate in growth rate between HL/LG and HL/HG at higher temperatures, suggesting that it survives better than HL/HG but lacks the rapid growth of HL/LG. The latter shows genomic markers for surviving oligotrophic conditions but may nonetheless be better equipped to utilize the higher nutrient environment of the mesotrophic and eutrophic lakes that these strains were originally isolated from.

Considering that not all strains of *M. aeruginosa* carry the *mcy* toxin operon whose product causes wildlife mortality and human illness, and that oligotrophic strains are more likely to carry functional *mcy* operons, our results suggest that future blooms that develop under climate warming may become more toxic and more tolerant of low-nutrient conditions [35]. This result is in-line with the growing evidence that cyanobacterial blooms are becoming more toxic through time [36,37]. However, the competitive dynamics in complex natural systems are multifactorial and challenging to predict from outcomes of controlled laboratory-based experiments, so additional investigation into whether oligotrophic strains will indeed become more prevalent in natural systems under climate warming should be further investigated. Furthermore, we acknowledge that, while our bacterial type groupings are supported by genomic evidence from our previous work (including a high-resolution phylogeny and genome-wide protein functional analyses), as well as a multivariate analysis in this study, our results nevertheless also highlight the level of between-strain variability found within these bacterial types [5]. Additional investigation to better parse and explain this inter- and intratype variation will be necessary to further expand and refine our understanding of these bacterial types of *M. aeruginosa*.

We previously documented the differential abundance of these three bacterial types of *M. aeruginosa* across a 20-fold gradient of TP in Michigan lakes [5]. Here, we show that this pattern of locally adapted bacterial types exists across a much larger region of lakes spanning the midwestern and eastern USA. Other cyanobacteria are also known to exhibit clades based on environmental conditions; for example, *Prochlorococcus* populations group into clades adapted to high- and low light intensity which occupy and exploit different depths of the euphotic zone in the ocean [38,39]. Furthermore, the major light intensity-adapted clades of *Prochlorococcus* are subdivided into further genomic subclades, several of which have evidence for adaptation to specific temperature ranges or/and nutrient conditions such as iron limitation [38,40]. For example, there is evidence that while the whole genome content within the HLII clade of *Prochlorococcus* is best explained by temperature, its phylogenetic subclades are most strongly linked to adaptation to P limitation [41]. The impressive diversity in these marine cyanobacteria is suggested to be a form of niche partitioning, allowing them to fill the many available microniches in the highly spatiotemporally variable ocean. In a similar manner, the bacterial types we previously described in *M. aeruginosa*, and find further evidence for in this study, are suggestive of adaptation to local niches in freshwater lakes, including both high and low phosphorus niches in eutrophic and mesotrophic lakes and the low phosphorus conditions of oligotrophic lakes [5]. As other cyanobacteria, such as *Prochlorococcus*, have been shown to have subclades adapted to differing temperature conditions within their major clades, it is conceivable that strains of *M. aeruginosa* grouped by our nutrient-limitation-based types may show considerable variation in their response to temperature. Indeed, our bacterial types do exhibit appreciable intratype variation. Still, with evidence of genome-wide functional similarity within types, such as adaptation to oligotrophic conditions among LG strains via genome streamlining and increased copies of phosphorus acquisition genes, paired with the clustering by bacterial type for growth and expression rate patterns that we observed within this study, our results suggest that for *M. aeruginosa* these types remain a useful and predictive means of categorization [5]. Nevertheless, future studies to better characterize intratype variation in temperature tolerance of *M. aeruginosa* clades will be essential to fully understand the complex environmental adaptation and future potential of *M. aeruginosa*.

While oligotrophic types have not yet been documented outside of North America, there is strong evidence that *M. aeruginosa* is capable of global dispersal. For example, early research on the biogeography of *M. aeruginosa* found no clear correlation between genetic and geographic distance, and although more recent research has identified patterns of genetic structure across spatial scales, the ability of *Microcystis* to disperse globally is well accepted [42–44]. Mechanisms of dispersal are thought to include aerosols, atmospheric bridges and both human- and wildlife-mediated dispersal [45–48]. Therefore, oligotrophic types might readily disperse into both inland waters previously uninhabited by *Microcystis* and those currently dominated by the eutrophic type. Such potentially rapid dispersal suggests that even if future environmental conditions caused by climate change and human activities cause mismatches between strains and lake conditions [34], these effects might be temporary with the rapid establishment of alternative bacterial types adapted to and capable of forming blooms under the new conditions.

To further investigate the mechanistic underpinnings of how each *M. aeruginosa* type tolerates warming, we analysed gene expression in the HSP gene family. In agreement with our growth rate and population persistence data, we found that the eutrophic and oligotrophic types responded differently in their expression patterns to warming. While all three types showed differential expression across the HSP gene family in response to warming, the magnitude of this heat shock response was substantially greater among oligotrophic types, as indicated by a significant type × temperature interaction in our statistical

model. These results provide a mechanistic foundation for the observed higher rates of population persistence of these types, suggesting that as the climate warms, either strains of the HL/HG type will have to adapt or may be outcompeted by the oligotrophic-adapted types.

While we found that bacterial type-specific responses to temperature were widespread across the HSP gene family, we found that two genes in particular, DnaK1 and Hsp20, showed contrasting responses between the oligotrophic and eutrophic types. The DnaK gene family, or HSP70 family, is a ubiquitous family of highly conserved molecular chaperones containing both constitutively expressed and stress-inducible forms [21]. Hsp20s, which belong to the small HSP family, are known for their strong induction by a variety of heat stresses [49,50]. Protein expression, both of constitutive HSPs as well as a diverse range of other proteins, are often downregulated during thermal stress due to slowing of translation as a whole and prioritized production of inducible forms of HSPs that are key for organismal survival during heat stress [51]. Our results suggest that oligotrophic types are more thermotolerant than the eutrophic type by maintaining elevated levels of constitutively expressed HSPs at warmer temperatures, as well as by substantially upregulating inducible HSPs, including DnaK1 and HSP20. However, there also remains appreciable intratype variation in gene expression. As previously discussed, some other cyanobacterial clades have been shown to contain subclades adapted to different temperatures. Therefore, while our motivation was to investigate type level trends in this study, an important future direction will be to further investigate intratype variation in thermotolerance. In summary, in addition to elevated expression by oligotrophic types of *M. aeruginosa* compared with the eutrophic type across most of the tested gene targets within the HSP family, we find highly type-specific responses to temperature in key members of both large and small HSPs responsible for mediating the heat shock response.

Our results share some similarities with prior work on the expression of HSPs in *M. aeruginosa* that found the upregulation of *HspA* and *HtpG* in response to heat and cold shocks [28]. Our warming experiment found a significant effect of temperature on *HtpG* expression, although not *HspA*. However, it should be noted that we used an acclimation approach to our warming study rather than a temperature shock. This probably elicits a different physiological response with those HSPs that respond rapidly to heat spikes typically different from those that respond to persistent high temperatures over long time periods.

We also found that temperature had a negative effect on the expression of *mcyE*, which is indicative of microcystin production in approximately 80% of cases [31]. However, our result contrasts with a recent meta-analysis that found a positive correlation between temperature and microcystin [36]. Additionally, we did not find a significant effect of bacterial type on the differential expression of *mcyE*. Based on prior work that had found the functional *mcy* operon to be more prevalent among oligotrophic types, we hypothesized that we might find greater expression responses of *mcyE* among these types [35]. While we did not find evidence to support this, nor the expected positive correlation between *mcy* operon gene expression and temperature, it is possible other conditions maintained during the study were not conducive to toxin production. For example, while the specific conditions that induce microcystin production are still debated, high-cell density and nutrient limitation are thought to be two important factors [52–55]. It is, therefore, conceivable that toxin production may have been relatively low either due to the lower cell densities in culture (thereby preventing activation of potential mechanisms for cell-density-dependent increased toxin production) or possible development of N limitation in month-old cultures (microcystin is an N-rich compound). It is also possible that we did not find differences in *mcyE* expression among bacterial types due to strain-by-strain variation within types, as others have found variation in microcystin production even between closely related strains [35]. Therefore, our lack of evidence for an effect of bacterial type on *mcyE* expression may be due to the complexity of *mcy* operon regulation.

There are several potential explanations for why oligotrophic types may be more thermotolerant. First, there is a precedence for a connection between genome streamlining and thermotolerance. Streamlining is a strategy involving both cellular and genome downsizing to allow more efficient use of sparse nutrients, with important ecological implications [56]. In thermophilic bacteria, both the size of the genome and the percentage of intergenic regions were found to be negatively correlated with the temperature at which the bacterial strain was found [57]. Similarly, we previously reported that LL/LG and HL/LG genomes contained a higher percentage of coding versus non-coding DNA, and therefore we could infer from Sabath *et al.* that these oligotrophic types might tolerate higher temperatures, as we do in fact find in the present study [5]. However, the authors hypothesized that the correlation was due to indirect selection for genome streamlining, driven by direct selection for smaller cell size at higher temperatures, as genome size is thought to constrain cell size. Yet, while we found multiple indicators of genome streamlining in the LL/LG type of *M. aeruginosa*, we did not find evidence for reduced genome size [5]. Furthermore, as *Microcystis* forms colonies that are frequently composed of  $10^4$ – $10^5$  cells, the functional implications of cell size versus colony size on temperature tolerance would need to be considered.

Another potential explanation for why oligotrophic types may be more thermotolerant is the co-occurrence of two notable selective pressures within cyanobacterial blooms. Late-stage blooms are typically characterized by both the depletion of bioavailable nutrients and warmer temperatures [58]. Such blooms typically develop later into the summer when atmospheric temperatures are higher [59,60]. Additionally, large cyanobacterial blooms are themselves heat traps, causing elevated local surface water temperatures [13]. Therefore, the streamlining of oligotrophic types may provide a selective advantage when exposed to two stressors that often occur simultaneously in late-stage blooms.

Last, an additional explanation for why oligotrophic types may be more thermotolerant stems from redundancy in cellular stress responses. While organisms inhabiting warmer environments are well known to have higher temperature thresholds for the induction of HSP expression, there is also evidence from a range of systems that populations adapted to extreme environments characterized by conditions other than warm temperatures also have an increased basal level of HSPs [23]. This can be explained by the fact that HSPs can be thought of as a more general response to stress overall [22,23]. For example, increased sodium levels in soils, which can cause osmotic stress, have been found to induce HSP expression in grasses [61]. Further, there is evidence that caloric limitation in eukaryotes can increase HSP responses [62]. Similarly, comparative work of

two species within the unicellular green algal genus *Chlamydomonas* found that *Chlamydomonas acidophila*, which is adapted to acidic environments, exhibited significantly higher levels of HSPs under control conditions compared with the more generalist *Chlamydomonas reinhardtii* [63]. Overall, it is conceivable that by evolving to a nutrient-limited environment, the LL/LG type may be more fine-tuned to respond to multiple types of stress or may be primed with higher constitutive levels of HSPs. A potential complication to this interpretation is genome streamlining within the LL/LG type, which may affect the number and expression of HSP family genes. Streamlined bacteria tend to have fewer sigma factors, which initiate transcription, and so could include a loss of sigma factors targeting HSPs and complex control of HSP expression. Ultimately, further research may elucidate what effects genome streamlining in bacteria may have on the regulation of HSPs. Nevertheless, the consistent growth rates that we observed in the LL/LG type across temperatures may be due to elevated constitutive levels of HSPs that are sufficient to mitigate any effects of temperature in laboratory cultures.

There are several important limitations to our study. First, our strains were not axenic (i.e. not free of heterotrophic bacteria) and so it is conceivable some results may differ with variation in the composition of the *M. aeruginosa* microbiome. It is also possible that some of the between strain variation we observe within bacterial types is due to differences in microbiome compositions between the strains. For example, our recent work found that *M. aeruginosa* has greater fitness and competitive ability when xenic [64]. Furthermore, we recently found that heterotrophic bacteria inhabiting the microbiome of oligotrophic types of *M. aeruginosa* share many of the same indicators of genome streamlining and features that facilitate survival in nutrient-depleted environments as had been found in their cyanobacterial hosts [26]. Therefore, differences in thermotolerance may also exist between the microbiomes of our *M. aeruginosa* types. Further, the complexity of natural systems is also expected to affect HSP expression. For example, heat shock response has been shown to be affected by light in some cyanobacteria [65]. Nevertheless, with increasing temperatures being the key feature of anthropogenic climate change, our results, which show responses to increased temperature with all other factors kept constant, should still provide valuable insight for predicting the effects of climate change on *Microcystis* and harmful bloom dynamics. Further, while not all inland waters are expected to reach the highest temperature tested in our study (32°C), one of the largest and deepest *Microcystis*-source lakes used in our study, oligotrophic Gull Lake (MI, USA), reached a 24 h epilimnetic mean temperature of 30°C as far back as 2012 [34]. Shallow eutrophic lakes, where *Microcystis* is more commonly found, have less thermal inertia and are likely to more readily achieve these extreme temperatures in the near future. Given the global distribution of *Microcystis*, these experimental temperatures are also highly applicable to subtropical and tropical environments. Finally, we note that a limitation to our study and classification system is the large variation that still exists between strains within bacterial types and our single biological replicate per strain per temperature condition. While these three types are well supported by genomic analysis in our previously published work, as well as the trait data in this study that shows significant clustering by bacterial type, future research should further consider and attempt to explain this intratype variability. For example, an expanded study with biological replication within strain could further clarify strain-by strain variation in temperature tolerance within bacterial types.

In conclusion, our results show that strains adapted to oligotrophy are better equipped to persist during warming scenarios, with higher or unchanged growth rates when comparing low to high temperature conditions. In contrast, strains adapted to eutrophic conditions tend to have lower persistence at higher temperatures. We fortify these results with gene expression data showing that different types of *M. aeruginosa* have differing patterns of expression of HSP genes in response to increased temperatures. Given previous research suggesting that oligotrophic strains are more likely to produce microcystin, a dangerous toxin, our results suggests that climate warming may select for the formation of cyanobacterial blooms with enhanced capacity to both produce the microcystin toxin and tolerate nutrient limitation. Therefore, intraspecific genetic diversity within *M. aeruginosa* may be key in predicting the dynamic of freshwater harmful algal blooms under climate warming.

**Ethics.** This work did not require ethical approval from a human subject or animal welfare committee.

**Data accessibility.** Metadata are archived in Dryad [66]. Sequences used for phylogenies are available at NCBI PQ666794-PQ666862.

**Declaration of AI use.** We have not used AI-assisted technologies in creating this article.

**Authors' contributions.** M.C.M.K.: data curation, formal analysis, investigation, methodology, visualization, writing—original draft, writing—review and editing; C.V.Q.: investigation; N.C.B.: investigation; W.D.: investigation; J.D.W.: conceptualization, data curation, formal analysis, funding acquisition, investigation, methodology, resources, supervision, writing—review and editing; S.L.J.: conceptualization, data curation, formal analysis, funding acquisition, investigation, methodology, resources, supervision, visualization, writing—review and editing.

All authors gave final approval for publication and agreed to be held accountable for the work performed therein.

**Conflict of interest declaration.** We declare we have no competing interests.

**Funding.** This project was supported by funding from the National Institutes of Health NIGMS R35GM142938 to S. L. Jackrel and a UCSD Starbucks Sustainability Solutions Research Scholarship to W. Ding.

**Acknowledgements.** We thank M. E. Jackrel, J. R. Dickey, A. Fabiani and T. Y. Broe for their constructive comments to improve this manuscript. We thank R. W. Bilich, C. L. Shaw and M. A. Duffy for assistance with water collection. We thank E. Perez-Coronel for assistance with optimizing the RNA extraction protocol, R. Y. Koch for assistance with RNA extractions, M. Fang for advice on qPCR experimental design and data analysis, and C. S. Spiegel for advice on statistical analysis.

## References

- Crutsinger GM, Collins MD, Fordyce JA, Gompert Z, Nice CC, Sanders NJ. 2006 Plant genotypic diversity predicts community structure and governs an ecosystem process. *Science* **313**, 966–968. (doi:10.1126/science.1128326)
- Whitham TG *et al.* 2006 A framework for community and ecosystem genetics: from genes to ecosystems. *Nat. Rev. Genet.* **7**, 510–523. (doi:10.1038/nrg1877)

3. Schopf JW. 2012 The fossil record of Cyanobacteria. In *Ecology of Cyanobacteria II: their diversity in space and time* (ed. BA Whitton), pp. 15–36. Dordrecht, The Netherlands: Springer. (doi:10.1007/978-94-007-3855-3\_2)
4. Whitton BA. 2012 *Ecology of Cyanobacteria II: their diversity in space and time*. Dordrecht, The Netherlands: Springer.
5. Jackrel SL, White JD, Evans JT, Buffin K, Hayden K, Sarnelle O, Deneff VJ. 2019 Genome evolution and host-microbiome shifts correspond with intraspecific niche divergence within harmful algal bloom-forming *Microcystis aeruginosa*. *Mol. Ecol.* **28**, 3994–4011. (doi:10.1111/mec.15198)
6. Huisman J, Codd GA, Paerl HW, Ibelings BW, Verspagen JMH, Visser PM. 2018 Cyanobacterial blooms. *Nat. Rev. Microbiol.* **16**, 471–483. (doi:10.1038/s41579-018-0040-1)
7. Hamilton DP, Wood SA, Dietrich DR, Puddick J. 2014 Costs of harmful blooms of freshwater cyanobacteria. In *Cyanobacteria*, pp. 245–256. John Wiley & Sons, Ltd. (doi:10.1002/9781118402238)
8. Paerl HW, Huisman J. 2009 Climate change: a catalyst for global expansion of harmful cyanobacterial blooms. *Environ. Microbiol. Rep.* **1**, 27–37. (doi:10.1111/j.1758-2229.2008.00004.x)
9. Jöhnk KD, Huisman J, Sharples J, Sommeijer B, Visser PM, Stroom JM. 2008 Summer heatwaves promote blooms of harmful cyanobacteria. *Glob. Chang. Biol.* **14**, 495–512. (doi:10.1111/j.1365-2486.2007.01510.x)
10. Coles JF, Jones RC. 2000 Effect of temperature on photosynthesis-light response and growth of four phytoplankton species isolated from a tidal freshwater river. *J. Phycol.* **36**, 7–16. (doi:10.1046/j.1529-8817.2000.98219.x)
11. Roberts RD, Zohary T. 1987 Temperature effects on photosynthetic capacity, respiration, and growth rates of bloom-forming cyanobacteria. *N. Z. J. Mar. Freshw. Res.* **21**, 391–399. (doi:10.1080/00288330.1987.9516235)
12. Hense I. 2007 Regulative feedback mechanisms in cyanobacteria-driven systems: a model study. *Mar. Ecol. Prog. Ser.* **339**, 41–47. (doi:10.3354/meps339041)
13. Kahru M, Leppanen JM, Rud O. 1993 Cyanobacterial blooms cause heating of the sea surface. *Mar. Ecol. Prog. Ser.* **101**, 1–7. (doi:10.3354/meps101001)
14. Harke MJ, Steffen MM, Gobler CJ, Otten TG, Wilhelm SW, Wood SA, Paerl HW. 2016 A review of the global ecology, genomics, and biogeography of the toxic cyanobacterium, *Microcystis* spp. *Harmful Algae* **54**, 4–20. (doi:10.1016/j.hal.2015.12.007)
15. Masango MG, Myburgh JG, Labuschagne L, Govender D, Bengis RG, Naicker D. 2010 Assessment of *Microcystis* bloom toxicity associated with wildlife mortality in the Kruger National Park, South Africa. *J. Wildl. Dis.* **46**, 95–102. (doi:10.7589/0090-3558-46.1.95)
16. Steffen MM *et al.* 2017 Ecophysiological examination of the Lake Erie *Microcystis* bloom in 2014: linkages between biology and the water supply shutdown of Toledo, OH. *Environ. Sci. Technol.* **51**, 6745–6755. (doi:10.1021/acs.est.7b00856)
17. Qin B, Zhu G, Gao G, Zhang Y, Li W, Paerl HW, Carmichael WW. 2010 A drinking water crisis in Lake Taihu, China: linkage to climatic variability and lake management. *Environ. Manag.* **45**, 105–112. (doi:10.1007/s00267-009-9393-6)
18. Wetzel RG. 2001 *Limnology: lake and river ecosystems*. San Diego, CA: Academic Press.
19. Scavia D *et al.* 2014 Assessing and addressing the re-eutrophication of Lake Erie: central basin hypoxia. *J. Great Lakes Res.* **40**, 226–246.
20. Parsell DA, Lindquist S. 1993 The function of heat-shock proteins in stress tolerance: degradation and reactivation of damaged proteins. *Annu. Rev. Genet.* **27**, 437–496. (doi:10.1146/annurev.ge.27.120193.002253)
21. Hartl FU, Bracher A, Hayer-Hartl M. 2011 Molecular chaperones in protein folding and proteostasis. *Nature* **475**, 324–332. (doi:10.1038/nature10317)
22. Lindquist S. 1986 The heat-shock response. *Annu. Rev. Biochem.* **55**, 1151–1191. (doi:10.1146/annurev.bi.55.070186.005443)
23. Feder ME, Hofmann GE. 1999 Heat-shock proteins, molecular chaperones, and the stress response: evolutionary and ecological physiology. *Annu. Rev. Physiol.* **61**, 243–282. (doi:10.1146/annurev.physiol.61.1.243)
24. White JD, Kaul RB, Knoll LB, Wilson AE, Sarnelle O. 2011 Large variation in vulnerability to grazing within a population of the colonial phytoplankton, *Microcystis aeruginosa*. *Limnol. Oceanogr.* **56**, 1714–1724. (doi:10.4319/lo.2011.56.5.1714)
25. Stemberger RS. 1981 A general approach to the culture of planktonic rotifers. *Can. J. Fish. Aquat. Sci.* **38**, 721–724. (doi:10.1139/f81-095)
26. Jackrel SL, White JD, Perez-Coronel E, Koch RY. 2023 Selection for oligotrophy among bacteria inhabiting host microbiomes. *mBio* **14**, e0141523. (doi:10.1128/mbio.01415-23)
27. Fortunato CS, Huber JA. 2016 Coupled RNA-SIP and metatranscriptomics of active chemolithoautotrophic communities at a deep-sea hydrothermal vent. *ISME J.* **10**, 1925–1938. (doi:10.1038/ismej.2015.258)
28. Rhee JS, Ki JS, Kim BM, Hwang SJ, Choi IY, Lee JS. 2012 HspA and HtpG enhance thermotolerance in the cyanobacterium, *Microcystis aeruginosa* NIES-298. *J. Microbiol. Biotechnol.* **22**, 118–125. (doi:10.4014/jmb.1108.08001)
29. Jungblut AD, Neilan BA. 2006 Molecular identification and evolution of the cyclic peptide hepatotoxins, microcystin and nodularin, synthetase genes in three orders of Cyanobacteria. *Arch. Microbiol.* **185**, 107–114. (doi:10.1007/s00203-005-0073-5)
30. Lu J, Struewing I, Wymer L, Tettenhorst DR, Shoemaker J, Allen J. 2020 Use of qPCR and RT-qPCR for monitoring variations of microcystin producers and as an early warning system to predict toxin production in an Ohio inland lake. *Water Res.* **170**, 115262. (doi:10.1016/j.watres.2019.115262)
31. Pacheco A, Guedes I, Azevedo S. 2016 Is qPCR a reliable indicator of cyanotoxin risk in freshwater? *Toxins* **8**, 172. (doi:10.3390/toxins8060172)
32. Cao H, Xu D, Zhang T, Ren Q, Xiang L, Ning C, Zhang Y, Gao R. 2022 Comprehensive and functional analyses reveal the genomic diversity and potential toxicity of *Microcystis*. *Harmful Algae* **113**, 102186. (doi:10.1016/j.hal.2022.102186)
33. Humbert JF *et al.* 2013 A tribute to disorder in the genome of the bloom-forming freshwater cyanobacterium *Microcystis aeruginosa*. *PLoS ONE* **8**, e70747. (doi:10.1371/journal.pone.0070747)
34. White JD, Sarnelle O, Hamilton SK. 2017 Unexpected population response to increasing temperature in the context of a strong species interaction. *Ecol. Appl.* **27**, 1657–1665. (doi:10.1002/eap.1558)
35. Berry MA, White JD, Davis TW, Jain S, Johengen TH, Dick GJ, Sarnelle O, Deneff VJ. 2017 Are oligotypes meaningful ecological and phylogenetic units? A case study of *Microcystis* in freshwater lakes. *Front. Microbiol.* **08**, 365. (doi:10.3389/fmicb.2017.00365)
36. Buley RP, Gladfelter MF, Fernandez-Figueroa EG, Wilson AE. 2022 Can correlational analyses help determine the drivers of microcystin occurrence in freshwater ecosystems? A meta-analysis of microcystin and associated water quality parameters. *Environ. Monit. Assess.* **194**, 493. (doi:10.1007/s10661-022-10114-8)
37. Heathcote AJ, Taranu ZE, Tromas N, MacIntyre-Newell M, Leavitt PR, Pick FR. 2023 Sedimentary DNA and pigments show increasing abundance and toxicity of cyanobacteria during the Anthropocene. *Freshw. Biol.* **68**, 1859–1874. (doi:10.1111/fwb.14069)
38. Biller SJ, Berube PM, Lindell D, Chisholm SW. 2015 *Prochlorococcus*: the structure and function of collective diversity. *Nat. Rev. Microbiol.* **13**, 13–27. (doi:10.1038/nrmicro3378)
39. Chen MY, Teng WK, Zhao L, Hu CX, Zhou YK, Han BP, Song LR, Shu WS. 2021 Comparative genomics reveals insights into cyanobacterial evolution and habitat adaptation. *ISME J.* **15**, 211–227. (doi:10.1038/s41396-020-00775-z)

40. Larkin AA, Blinbery SK, Howes C, Lin Y, Loftus SE, Schmaus CA, Zinser ER, Johnson ZI. 2016 Niche partitioning and biogeography of high light adapted *Prochlorococcus* across taxonomic ranks in the North Pacific. *ISME J.* **10**, 1555–1567. (doi:10.1038/ismej.2015.244)
41. Ustick LJ, Larkin AA, Martiny AC. 2023 Global scale phylogeography of functional traits and microdiversity in *Prochlorococcus*. *ISME J.* **17**, 1671–1679. (doi:10.1038/s41396-023-01469-y)
42. van Gremberghe I, Leliaert F, Mergeay J, Vanormelingen P, Van der Gucht K, Debeer AE, Lacerot G, De Meester L, Vyverman W. 2011 Lack of phylogeographic structure in the freshwater cyanobacterium *Microcystis aeruginosa* suggests global dispersal. *PLoS One* **6**, e19561. (doi:10.1371/journal.pone.0019561)
43. Moreira C, Spillane C, Fathalli A, Vasconcelos V, Antunes A. 2014 African origin and Europe-mediated global dispersal of the cyanobacterium *Microcystis aeruginosa*. *Curr. Microbiol.* **69**, 628–633. (doi:10.1007/s00284-014-0628-2)
44. Shirani S, Hellweger FL. 2017 Neutral evolution and dispersal limitation produce biogeographic patterns in *Microcystis aeruginosa* populations of lake systems. *Microb. Ecol.* **74**, 416–426. (doi:10.1007/s00248-017-0963-5)
45. Sharma NK, Singh S. 2010 Differential aerosolization of algal and cyanobacterial particles in the atmosphere. *Indian J. Microbiol.* **50**, 468–473. (doi:10.1007/s12088-011-0146-x)
46. Lewandowska AU, Śliwińska-Wilczewska S, Woźniczka D. 2017 Identification of cyanobacteria and microalgae in aerosols of various sizes in the air over the southern Baltic Sea. *Mar. Pollut. Bull.* **125**, 30–38. (doi:10.1016/j.marpolbul.2017.07.064)
47. Doblin MA, Coyne KJ, Rinta-Kanto JM, Wilhelm SW, Dobbs FC. 2007 Dynamics and short-term survival of toxic cyanobacteria species in ballast water from NOBOB vessels transiting the Great Lakes—implications for HAB invasions. *Harmful Algae* **6**, 519–530. (doi:10.1016/j.hal.2006.05.007)
48. Curren E, Leong SCY. 2020 Natural and anthropogenic dispersal of cyanobacteria: a review. *Hydrobiologia* **847**, 2801–2822. (doi:10.1007/s10750-020-04286-y)
49. Basha E, O'Neill H, Vierling E. 2012 Small heat shock proteins and  $\alpha$ -crystallins: dynamic proteins with flexible functions. *Trends Biochem. Sci.* **37**, 106–117. (doi:10.1016/j.tibs.2011.11.005)
50. Srivastava AK, Rai AN, Neilan BA. 2013 *Stress biology of cyanobacteria: molecular mechanisms to cellular responses*. Boca Raton, FL: CRC Press.
51. Klaips CL, Jayaraj GG, Hartl FU. 2018 Pathways of cellular proteostasis in aging and disease. *J. Cell Biol.* **217**, 51–63. (doi:10.1083/jcb.201709072)
52. Horst GP, Sarnelle O, White JD, Hamilton SK, Kaul RB, Bressie JD. 2014 Nitrogen availability increases the toxin quota of a harmful cyanobacterium, *Microcystis aeruginosa*. *Water Res.* **54**, 188–198. (doi:10.1016/j.watres.2014.01.063)
53. Pimentel JSM, Giani A. 2014 Microcystin production and regulation under nutrient stress conditions in toxic *Microcystis* strains. *Appl. Environ. Microbiol.* **80**, 5836–5843. (doi:10.1128/aem.01009-14)
54. Wang S, Ding P, Lu S, Wu P, Wei X, Huang R, Kai T. 2021 Cell density-dependent regulation of microcystin synthetase genes (*mcy*) expression and microcystin-LR production in *Microcystis aeruginosa* that mimics quorum sensing. *Ecotoxicol. Environ. Saf.* **220**, 112330. (doi:10.1016/j.ecoenv.2021.112330)
55. Wood SA, Puddick J, Hawes I, Steiner K, Dietrich DR, Hamilton DP. 2021 Variability in microcystin quotas during a *Microcystis* bloom in a eutrophic lake. *PLoS One* **16**, e0254967. (doi:10.1371/journal.pone.0254967)
56. Giovannoni SJ, Cameron Thrash J, Temperton B. 2014 Implications of streamlining theory for microbial ecology. *ISME J.* **8**, 1553–1565. (doi:10.1038/ismej.2014.60)
57. Sabath N, Ferrada E, Barve A, Wagner A. 2013 Growth temperature and genome size in bacteria are negatively correlated, suggesting genomic streamlining during thermal adaptation. *Genome Biol. Evol.* **5**, 966–977. (doi:10.1093/gbe/evt050)
58. Sarnelle O. 1992 Contrasting effects of *Daphnia* on ratios of nitrogen to phosphorus in a eutrophic, hard-water lake. *Limnol. Oceanogr.* **37**, 1527–1542. (doi:10.4319/lo.1992.37.7.1527)
59. Sommer U. 1989 The role of competition for resources in phytoplankton succession. In *In plankton ecology: succession in plankton communities* (ed. U Sommer), pp. 57–106. Berlin, Germany: Springer. (doi:10.1007/978-3-642-74890-5\_3)
60. De Senerpont Domis LN, Mooij WM, Huisman J. 2007 Climate-induced shifts in an experimental phytoplankton community: a mechanistic approach. In *Shallow lakes in a changing world* (eds RD Gulati, E Lammens, N De Pauw, E Van Dock), pp. 403–413. Dordrecht, The Netherlands: Springer. (doi:10.1007/978-1-4020-6399-2\_36)
61. Hamilton EW III, McNaughton SJ, Coleman JS. 2001 Molecular, physiological, and growth responses to sodium stress in C 4 grasses from a soil salinity gradient in the Serengeti ecosystem. *Am. J. Bot.* **88**, 1258–1265. (doi:10.2307/3558337)
62. Moura C, Lollo P, Morato P, Amaya-Farfan J. 2018 Dietary nutrients and bioactive substances modulate heat shock protein (HSP) expression: a review. *Nutrients* **10**, 683. (doi:10.3390/nu10060683)
63. Gerloff-Elias A, Barua D, MÄllich A, Spijkerman E. 2006 Temperature- and pH-dependent accumulation of heat-shock proteins in the acidophilic green alga *Chlamydomonas acidophila*. *FEMS Microbiol. Ecol.* **56**, 345–354. (doi:10.1111/j.1574-6941.2006.00078.x)
64. Schmidt KC, Jackrel SL, Smith DJ, Dick GJ, Denef VJ. 2020 Genotype and host microbiome alter competitive interactions between *Microcystis aeruginosa* and *Chlorella sorokiniana*. *Harmful Algae* **99**, 101939. (doi:10.1016/j.hal.2020.101939)
65. Asadulghani Suzuki Y, Nakamoto H. 2003 Light plays a key role in the modulation of heat shock response in the cyanobacterium *Synechocystis* sp PCC 6803. *Biochem. Biophys. Res. Commun.* **306**, 872–879. (doi:10.1016/s0006-291x(03)01085-4)
66. Jackrel S, Kuijpers M. 2024 Data from: Intraspecific divergence within *Microcystis aeruginosa* mediates the dynamics of freshwater harmful algal blooms under climate warming scenarios. Dryad Digital Repository. ()

# Supplementary Information

## Intraspecific divergence within *Microcystis aeruginosa* mediates the dynamics of freshwater harmful algal blooms under climate warming scenarios

Mirte C. M. Kuijpers<sup>1</sup>, Catherine V. Quigley<sup>2</sup>, Nicole C. Bray<sup>2</sup>, Wenbo Ding<sup>1</sup>, Jeffrey D. White<sup>2</sup>, Sara L. Jackrel<sup>1\*</sup>

<sup>1</sup> Department of Ecology, Behavior and Evolution, School of Biological Sciences, University of California San Diego, La Jolla, California, USA

<sup>2</sup> Department of Biology, Framingham State University, Framingham, Massachusetts, USA

\*Corresponding author: [sjackrel@ucsd.edu](mailto:sjackrel@ucsd.edu)

Proceedings of the Royal Society B

DOI: 10.1098/rspb.2024.2520

## Supplementary Methods

### *Gene count analysis*

As tolerance to heat stress can be the consequence of both variation in gene copy number and expression, we first surveyed whether the three bacterial types of *M. aeruginosa* varied in copy number for genes associated with heat shock proteins. Forty-six metagenome-assembled genomes including 18 LL/LG, 11 HL/LG and 17 HL/HG MAGs, as described in our prior work, were annotated using the Joint Genome Institutes Genomes OnLine Database (JGI GOLD) following standard pipelines<sup>[1,2]</sup>. We used keyword searches in JGI GOLD to survey the frequency of twenty genes associated with the synthesis of common heat shock proteins, including the HSP and Clp proteins.

### *Strain Genotyping and Phylogenetics*

We previously identified the three types of *M. aeruginosa* used in this study using a multi-locus sequence typing (MLST) analysis of five marker genes<sup>[3,4]</sup>. While accurate, this method requires a substantial sequencing effort that reduces its scalability. We therefore aimed to determine whether the rRNA-ITS region, which has been shown to provide high resolution strain discrimination for *M. aeruginosa*, could be used as an inexpensive and scalable alternative to accurately distinguish between high- and low-nutrient bacterial types. This method has successfully been used for distinguishing clades and ecotypes in the cyanobacterium *Prochlorococcus*, which also has distinct bacterial types delimited by various environmental/niche adaptations<sup>[5,6]</sup>. As opposed to our MLST analysis, which required ~ nine kilobases, an ITSc analysis requires less than 500 base pairs. To test whether the rRNA-ITSc and MLST methods are comparable in accuracy, we used our previously published shotgun metagenomic dataset of 46 strains of *M. aeruginosa* originating from inland lakes of Michigan to construct a phylogeny using both methods. Each of the five house-keeping genes for each strain had previously been located within this metagenomic dataset as described in<sup>[2]</sup>. To locate the rRNA-ITSc region for each strain in the dataset, we used a representative sequence of the *M. aeruginosa* rRNA-ITSc to search for and extract gene orthologs by making custom blast databases and using the `blastdbcmd` command to extract sequence ranges based on blast output coordinates. As we found high accuracy of the rRNA-ITSc method to distinguish between the high and low-nutrient bacterial types, described in detail in

supplementary results and Fig. S1, we proceeded with this approach for each of the strains that we isolated in 2019. We amplified the rRNA-ITS<sub>c</sub> region of *M. aeruginosa* biomass via colony PCR using the CSIF and ULR primers as described in Janse et al. 2003. All colony PCR reactions and Sanger sequencing were completed in 2020 for each of our 24 recently isolated *M. aeruginosa* strains through Azenta Life Sciences (South Plainfield, NJ).

To construct phylogenies, we compiled extracted gene sequences that we obtained from our previously published shotgun metagenomic dataset (46 strains) with the Sanger sequences that we obtained for our 24 newly isolated strains of *M. aeruginosa*, aligned sequences with MUSCLE using default parameters and trimmed alignments using Geneious. Consensus sequences and alignments were reviewed manually to ensure accuracy and final alignment lengths were 490, 8954, and 518 base pairs for the phylogenies reported in Fig 1 using the ITS<sub>c</sub> method, Fig S1A using the MLST method and Fig S1B using the ITS<sub>c</sub> method, respectively. We constructed phylogenies using RAxML version 8.2.12 with an outgroup of *Synechococcus* strain NC 006576 obtained from NCBI, and a GTRGAMMA evolutionary model with bootstrap analyses of 10,000 repetitions to search for the best-scoring maximum likelihood tree. All phylogenetic trees were illustrated using ggTree<sup>[7]</sup>. Strains isolated in this study were assigned their bacterial type based on the strain's position within the phylogenetic tree (shown in Fig 1) and the TP of the lake from which each strain was isolated. We used standard thresholds in TP for assigning trophic state with an oligotrophic-mesotrophic boundary of 10 µg/L and a mesotrophic-eutrophic boundary of 30 µg/L<sup>[8]</sup>. We note that the oligotrophic lakes in our study have appreciable densities of *Microcystis* due to the introduction of invasive dreissenid mussels<sup>[9,10]</sup>.

### **Gene expression analysis**

RNA was obtained via phenol-chloroform extraction with the Invitrogen *mirVana*<sup>TM</sup> miRNA Isolation Kit using a protocol modified by Fortunato and Huber (Fortunato & Huber, 2016). In brief, we added half of a 23 mm filter containing the algal biomass into MP Biomedicals<sup>TM</sup> Lysing Matrix E 2 mL tubes with 750 µl of Lysis/Binding Buffer from the *mirVana*<sup>TM</sup> miRNA Isolation Kit. We vortexed tubes for 10 min, added 10 µl of miRNA Homogenate Additive, incubated for 10 minutes on ice, and centrifuged at 4,000 g for 2 minutes at 4°C. We transferred lysates to clean 1.5 ml tubes and repeated centrifugation to transfer any remaining lysate to the same 1.5 ml tube. We added 1-part acid-phenol chloroform to sample lysate to each tube, inverted a few times, and centrifuged for 5 minutes at 10,000 g. We removed the top aqueous layer, transferred to a new 1.5 ml tube, and from this point onwards followed the Total RNA isolation Procedure published for the *mirVana*<sup>TM</sup> miRNA Isolation Kit without any further modifications. Final RNA concentrations were measured with an Invitrogen Qubit 4 Fluorometer. We note that we were unable to successfully extract RNA from all samples, despite multiple attempts, likely due to some populations experiencing major decline during the warming trials, leading to low collected biomass for these populations.

cDNA was synthesized from the extracted RNA using the SuperScript III First-Strand Synthesis System with random hexamer primers, 8 µL RNA per reaction and 4 reactions pooled per sample. We followed the default procedure in all aspects, except in adding 4x the volume of all components, including the RNA input, for each sample such that the default ratio of each component to each other component and the sample was maintained throughout the protocol. This yielded 4x the final product, which was required to allow qPCR with multiple primers, each with their own technical replicates. The final product cDNA was either stored at -20°C or was used immediately for qPCR.

When quantifying gene expression using qPCR, each sample had reactions for all 14 primers and two sets of negative controls simultaneously run in the same plate with a

minimum of four technical replicates per primer. To ensure our expression results were primarily indicative of the host and not associated heterotrophic bacteria, we verified that all primers matched predominantly to *Microcystis spp.* using NCBI Primer-Blast against the nr nucleotide database. We followed the default 10  $\mu$ L reaction volume PowerTrack™ SYBR™Green Master Mix protocol of 1  $\mu$ L sample cDNA, 5  $\mu$ L master mix, 0.5  $\mu$ L of forward and reverse primers each, and 3.25  $\mu$ L nuclease-free water without the addition of the optional Yellow Sample Buffer. We replaced sample cDNA with distilled nuclease-free water for our negative controls. Each plate always contained one set of negative controls with our reference primer set (*rpoA* forward and reverse) and another set of negative controls with a different primer set from our other 13 primer sets. Plates were run on a CFX96™-RealTimeSystem-C1000-Touch™ Thermal Cycler with the PowerTrack ‘fast’ program: 95°C for 2 min, followed by 40 cycles of 15s at 95°C and 60s at 60°C, followed by the ‘fast’ dissociation step program to create a melting curve from the PowerTrack protocol. Raw data was processed using the CFX Maestro™ software to determine Ct values via linear regression.

Differential gene expression was determined using the  $2^{-\Delta\Delta C_t}$  method<sup>[11]</sup>, with 20°C as the baseline control treatment and *rpoA* as the reference gene. To calculate this  $2^{-\Delta\Delta C_t}$  metric, all NAs were set to 40, the maximum CT possible in our runs. For two HL/HG strains, FA19-02 and F19-02, and one LL/LG strain, G19-02, we were unable to successfully extract RNA for the 20°C condition. Therefore, we used an average of the CT value for each target at the 20°C conditions for all the other strains of the matching bacterial type as a replacement for the CT value for each target for the FA19-02, F19-02 and G19-02 strains at 20°C. Efficiencies were assessed by a visual comparison, with all sharing a similar shape and their slopes approximately parallel. Additionally, we restrict all statistical comparisons to within a single gene target, so any variation across gene targets in the efficiency of reverse transcription or qPCR should not bias our reported results.

### ***Statistics***

Growth rates of *M. aeruginosa* cultures were determined as the slope of the linear regression of ln-transformed chlorophyll-*a* versus time and then boxcox transformed to improve normality for the linear models. We first determined whether growth rates for the first week (exponential phase) of growth were dependent on bacterial type and temperature using a linear mixed effects model with type, temperature, and their interaction as fixed effects and strain as a random effects term. We then determined whether growth rates over the course of the full four-week incubation were dependent on bacterial type and temperature using a linear mixed effects model with type, temperature, and their interaction as fixed effects and growth time point nested within strain as a random effects term. We also repeated this analysis with growth time point as a fixed effect. For the full four-week model we also utilized Tukey post-hoc comparisons.

In addition, we evaluated growth rates of each bacterial type in response to temperature using hierarchical general additive models as outlined in Pedersen *et al.* 2019<sup>[12]</sup>. This modeling framework does not have an assumption of linearity. We used a Gaussian error distribution using the mgcv package<sup>[13]</sup> for both the exponential phase and full four-week dataset. Briefly, for each dataset we built a baseline model *G* which contained only a global trendline for the effect of temperature on growth rate across all strains; a model *GS* that allowed variation from that global trend in shape but not smoothness for each *M. aeruginosa* type; a model *GI* which also allowed variation in smoothness from the global trend for each type; a model *S* that allowed a different response curve with similar smoothness for each type and had no global trendline to constrain type-specific curve shapes to; and a model *I* that allowed a different response curve for each type in terms of both shape

and smoothness with no global trendline to constrain either. We then performed AIC based model selection, with the selection criteria for each successive model to be at least 2 AIC points lower in score than the next most conservative model previously accepted, where model conservativeness  $G > GS > GI > S > I$  (see Table S2). In summary, for a model other than G to be selected it was required to have an AIC at least 2 points lower than G, and every other model more conservative than it that was accepted in a previous step of model selection. We report the results of the best model for exponential phase, the four-week study with phase as a random effect, and the four-week study with phase as a fixed factor, to confirm that our results were not dependent on the assumption of a linear response of growth rate to temperature.

Finally, we determined whether population persistence over the course of the study was dependent on type and temperature using a cumulative link mixed effects model (clmm), which is designed for ordinal response variables. We defined population persistence as those cultures displaying a positive growth rate, whereas a ‘non-persisting’ declining population displayed a negative growth rate. Consistent with the structure of our linear mixed effects model used for growth rates, our clmm for population persistence used type, temperature, and their interaction as fixed effects and growth time point and strain as random effects. We also evaluated each *M. aeruginosa* type independently using linear mixed effects models with temperature as a fixed effect and strain as a random effects term.

Next, we analyzed whether gene expression of heat shock proteins was significantly different between bacterial types and/or significantly affected by the temperature treatments. We used a *boxcox* transformation to improve normality for our measure of relative gene expression ( $2^{-\Delta\Delta Ct}$ )<sup>[14]</sup>. We first determined whether relative gene expression was dependent on type and temperature using a linear mixed effects model with type, temperature and their interactions as fixed effects and gene target nested within strain as a random effect term. We then used the same model framework to test each gene target individually. All models were created using the *lme*, *gam* and *clmm* functions from the *nmle*, *mgecv* and *ordinal* packages in R<sup>[13,15-18]</sup>. Tukey post-hoc comparisons were completed using the *emmeans* package in R<sup>[19]</sup>. Finally, to test whether the strains within bacterial types showed similar patterns across both growth and expression dynamics (for all temperatures except the baseline 20°C to allow calculation of relative gene expression), we used a MANOVA followed by a Linear Determinants Analysis<sup>[20]</sup>. All figures were made with the *ggplot2* package, with the exception of the phylogenies and maps, which were made with *ggTree* and *qGIS* with the Natural Earths dataset, respectively<sup>[7,21,22]</sup>. To aid in visualization of our qPCR data, we used the *coord\_cartesian* function within *ggplot2* to center the boxplots without affecting data distributions.

## **Supplementary Results**

We found that our newly constructed phylogeny from rRNA-ITSc sequences recapitulates the patterns of high-nutrient versus low-nutrient bacterial types that we had previously identified in our original phylogeny constructed using a multi-locus sequence typing analysis (MLST) with five marker genes (Fig. S1). Specifically, the identical strains were grouped into the high versus low types irrespective of using the rRNA-ITSc or MLST method, with similar confidence levels for the node separating these two groups (Fig. S1, bootstrapping value of 85% for MLST versus 72% for ITSc method). While the ITSc approach alone could not distinguish between the LL/LG and HL/LG types, categorization could still be completed accurately by using phylogenetic positioning to determine low versus high genotype combined with trophic status of the lake of origin to determine low versus high nutrient lake (Table S1).

## Supplementary Figures

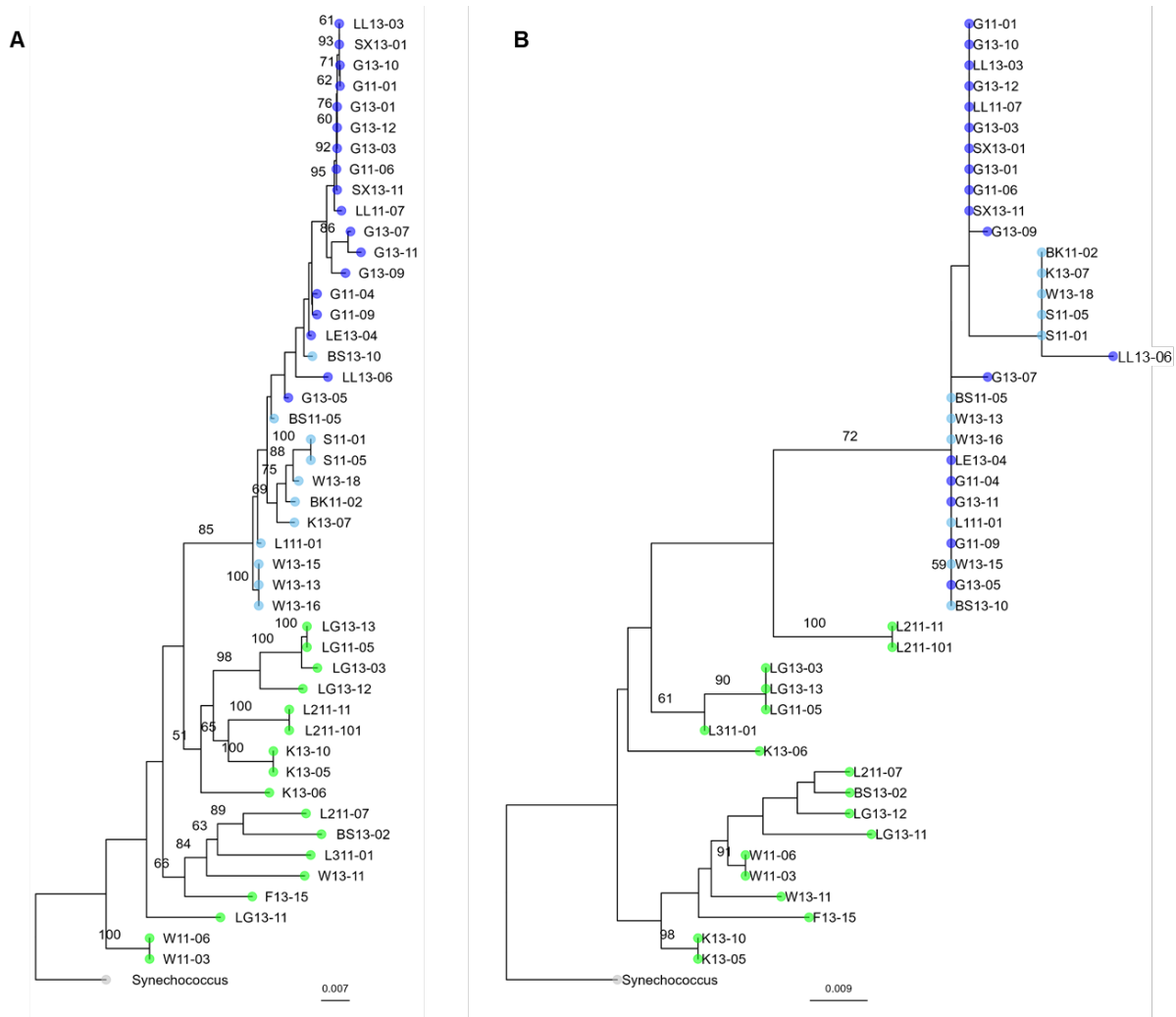


**Fig S1.** Similar phylogenetic structure of the three bacterial types of *M. aeruginosa* originally described in Jackrel et al. 2019 using a multi-locus sequence typing analysis can be obtained from using the rRNA-ITSc region. Phylogeny includes 46 isolates of *M. aeruginosa* collected from 14 inland lakes of Michigan, USA, as well as the cyanobacterium *Synechococcus* as an outgroup comparison. A) Multi-locus sequence typing analysis reproduced from Jackrel et al. 2019 by constructing a phylogeny with RAxML based on five housekeeping genes (*ftsZ*, *glnA*, *gltX*, *gyrB* and *pgi*). B) Phylogeny based only on the rRNA-ITSc region, as described by Janse et al. 2003, extracted from shotgun metagenomic sequences of isolates. The three bacterial types of *M. aeruginosa* are depicted as those originating from oligotrophic lakes in dark blue, i.e. the LL/LG type; those originating from eutrophic and mesotrophic lakes that clustered with oligotrophic lakes, i.e. the HL/LG type in light-blue; and all other isolates originating from eutrophic and mesotrophic lakes, i.e. the HL/HG type in green.

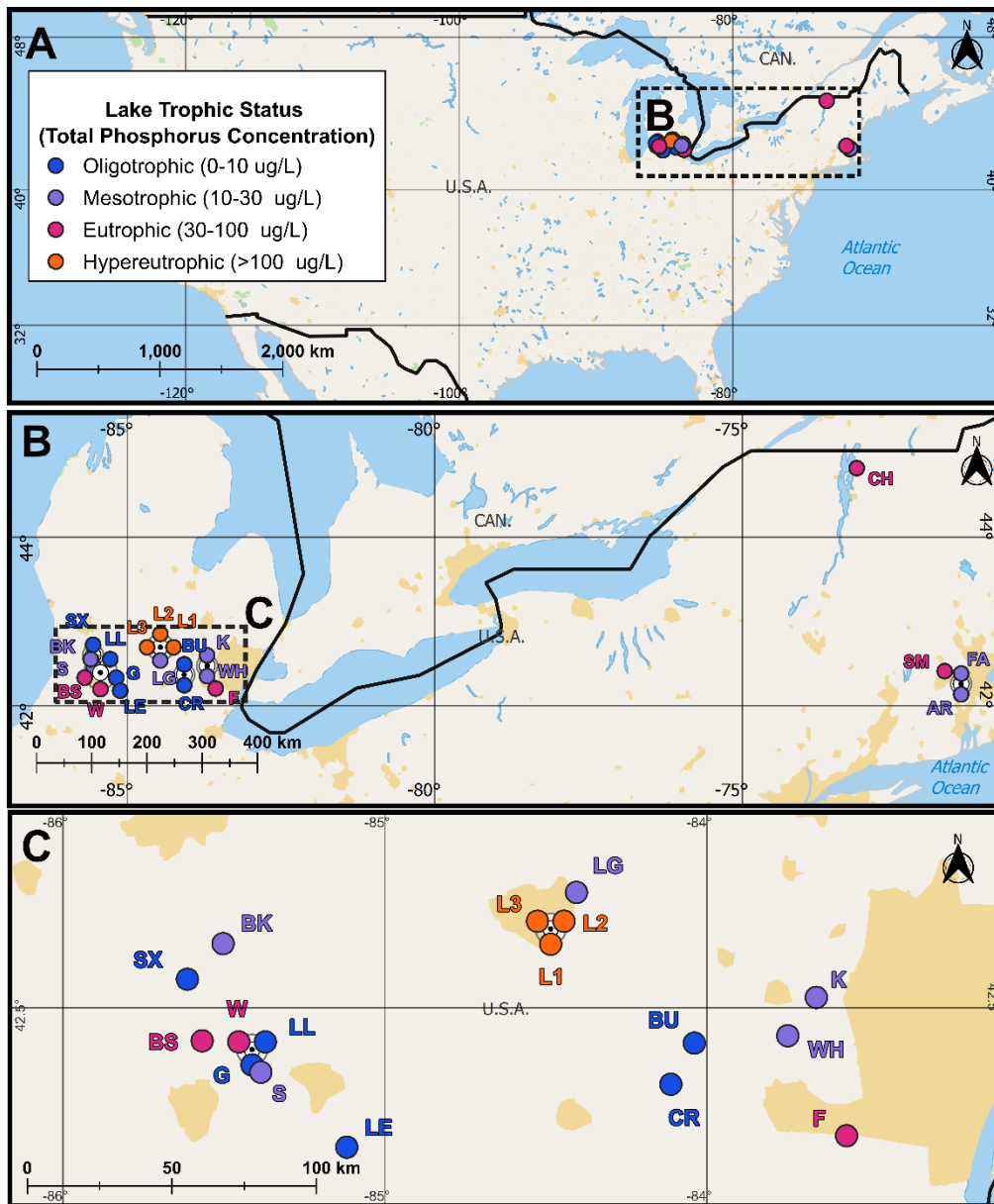


**Figure S2.** Geographic placement of the lakes from which the *M. aeruginosa* strains were isolated for both the new isolates and previously collected *M. aeruginosa* strain datasets. Lake symbols are colored by average total Phosphorus ( $\mu\text{g/L}$ ), see Table S1 for further details on these lakes. This figure was created with qGIS using data from the Natural Earth Data datasets.

**Table S1.** Associated metadata for all strains of *M. aeruginosa* originating from lakes in midwestern and northeastern USA. Strains include those used only for the phylogenetic analyses as well as those used for the warming experiment. New isolate strains that were sequenced but not used in the phylogeny due to poor quality are in italics while new isolate strains that were both sequenced and used in the warming experiment are in bold.

Lake/Location	Latitude, Longitude	Mean Total Phosphorus (TP) (µg/L)	TP range (µg/L)	# of TP measurements	Years Sampled	Mean Chl-a (µg/L)	Mean SRP (µg/L)	Mean NH4 (µg/L)	Mean NOs (µg/L)	Strains Isolated	Genotype Isolated
Ashland Reservoir, Middlesex Co., MA, USA	42.244289, -71.461792	13.6	8.2 - 20.2	23	2015-2019	5.4	4.9	49.9	57.8	<b>AR19-01</b> , <i>AR19-02</i>	HL/LG
Baker Lake, Barry Co., MI, USA	42.64643, -85.50279	28.0	11.5 - 54.6	4	2009, 2011, 2013	33.8	4.6	34.9	52.3	BK11-02	HL/LG
Baseline Lake, Allegan Co., MI, USA	42.42421, -85.5677	36.1	24.7 - 48.0	6	1998-1999, 2009, 2011, 2013	47.1	3.6	19.0	31.1	BS11-05, BS13-02, BS13-10	HL/LG, HL/HG
Bruin Lake, Washtenaw Co., MI, USA	42.418874, -84.039033	5.83	3.9-6.79	10	2007, 2011-2015, 2019	1.33	0.60	19.83	0.171	<b>BU19-01</b> , <b>BU19-02</b> , BU19-03, <b>BU19-04</b>	LL/LG
Crooked Lake, Washtenaw Co., MI, USA	42.324493, -84.111899	6.5	1.0-10.0	4	2002, 2007, 2019	ND	ND	ND	ND	<b>CR19-01</b> , <b>CR19-02</b> , CR19-03, <i>CR19-04</i> , CR19-05, <b>CR19-06</b>	LL/LG
Farm Pond, Middlesex Co., MA, USA	42.279281, -71.422882	18.8	8.8-35.2	14	2015-2019	4.2	3.8	35.6	37.3	FA19-01, <b>FA19-02</b> , FA19-03, FA19-04, <b>FA19-05</b> , <b>FA19-06</b>	HL/HG
Ford Lake, Washtenaw Co., MI, USA	42.20619, -83.566	65.0	44.8 - 99.6	5	2009, 2011, 2013, 2016, 2019	56.2	10.2	465.1	514.0	F19-01, <b>F19-02</b> , F19-03, <i>F19-04</i> , F13-15	HL/HG
Gull Lake, Barry / Kalamazoo Co., MI, USA	42.39651, -85.40936	7.6	2.3-13.1	201	1998-2014	3.7	1.3	22.1	277.0	<b>G19-01</b> , <b>G19-02</b> , G19-04, G11-01, G11-04, G11-06, G11-09, G13-01, G13-03, G13-05, G13-07, G13-09, G13-10, G13-12	LL/LG
Kent Lake, Oakland Co., MI, USA	42.52346, -83.66	23.6	15.2 - 31.5	3	2009, 2013	23.1	3.3	67.2	44.4	K13-05, K13-06, K13-07, K13-10	HL/LG, HL/HG
Lake Champlain-St. Albans Bay, Franklin Co., VT, USA	44.804592, -73.139215	33.3	14.5 - 72.6	98	2015-2019	ND	ND	ND	ND	<b>CH19-02</b> , CH19-03	HL/LG
Lake Lansing, Ingham Co., MI, USA	42.76324, -84.405	17.1	16.6 - 17.6	2	2011, 2013	5.5	5.1	11.1	89.0	LG11-05, LG13-02, LG13-03, LG13-11, LG13-1	HL/HG
Lee Lake, Calhoun Co., MI, USA	42.17991, -85.11844	9.0	3.4 - 13.2	5	2003, 2009, 2011, 2013	4.0	1.9	5.3	40.4	LE13-04	LL/LG
Little Long Lake, Barry Co., MI, USA	42.41803, -85.44348	8.0	3.2 - 13.4	42	2011 - 2014	4.1	1.0	100.0	312.5	LL11-07, LL13-03, LL13-6	LL/LG
MSU lake 1, Ingham Co., MI, USA	42.68059, -84.4831	163.5	71.0 - 209.9	3	2009, 2011, 2013	12.2	155.8	42.5	134.5	L111-01	HL/LG
MSU lake 2, Ingham Co., MI, USA	42.68059, -84.4871	196.8	105.3 - 456.2	79	2009-2013	240.8	7.3	6.8	157.6	L211-07, L211-01, L211-11	HL/HG
MSU lake 3, Ingham Co., MI, USA	42.67928, -84.4849	128.7	115.4 - 153.0	3	2011, 2013	53.3	4.1	9.4	543.7	L311-01	HL/HG
Sherman Lake, Kalamazoo Co., MI, USA	42.35212, -85.38545	13.7	4.8-24.0	4	2009, 2011, 2013	9.1	2.8	0.0	64.9	S11-01, S11-05	HL/LG
Sixteen Lake, Allegan Co., MI, USA	42.56518, -85.61352	8.8	6.4 - 10.6	3	2009, 2013	5.0	1.0	127.5	1917.6	SX13-01, SX13-11	LL/LG
South Meadow Pond, Worcester Co., MA, USA	42.415042, -71.709673	50.7	NA	1	2019	16.7	20.0	49.9	ND	<b>SM19-01</b> , <i>SM19-02</i> , <b>SM19-03</b> , <b>SM19-04</b>	HL/HG, HL/LG
Whitmore Lake, Livingston County, MI, USA	42.435690, -83.748680	12.69	4.9 - 16.58	5	2007, 2009, 2014, 2019	4.38	0.34	2.44	0.165	<b>WH19-01</b> , <b>WH19-02</b> , WH19-03, <b>WH19-04</b> , WH19-05	HL/HG, HL/LG
Wintergreen Lake, Kalamazoo Co., MI, USA	42.39757, -85.38536	47.8	26.2 - 92.1	4	2009, 2011, 2013	21.4	2.7	236.0	129.7	W11-03, W11-06, W13-11, W13-13, W13-15, W13-16, W13-18	HL/LG, HL/HG

**Table S2.** AIC scores for GAM selection for both the exponential phase only and full four-week dataset models (for the latter both with and without Phase as a random effect). Model terminology (G, GS, GI, I and S) come from ref<sup>[12]</sup>. For each model selection procedure, the selected model is marked with a \*. Model conservativeness, from highest to lowest is  $G > GS > GI > S > I$ . For exact model details please see the code provided in the supplementary materials package.

<b>Dataset</b>	<b>Model</b>	<b>Random effects</b>	<b>df</b>	<b>AIC</b>	<b><math>\Delta</math>AIC from most conservative model (G)</b>
Exponential phase only	G	Strain	12	-61	0
Exponential phase only	GS*	Strain	17	-70	9
Exponential phase only	GI	Strain	18	-71	10
Exponential phase only	S	Strain	15	-67	6
Exponential phase only	I	Strain	19	-62	1
Full four-weeks	G	Strain, Phase	13	-155	0
Full four-weeks	GS*	Strain, Phase	10	-165	10
Full four-weeks	GI	Strain, Phase	15	-153	+2
Full four-weeks	S	Strain, Phase	10	-164	9
Full four-weeks	I	Strain, Phase	16	-154	+1
Full four-weeks	G	Strain	19	-150	0
Full four-weeks	GS	Strain	17	-160	10
Full four-weeks	GI	Strain	17	-151	1
Full four-weeks	S*	Strain	13	-162	12
Full four-weeks	I	Strain	18	-152	2

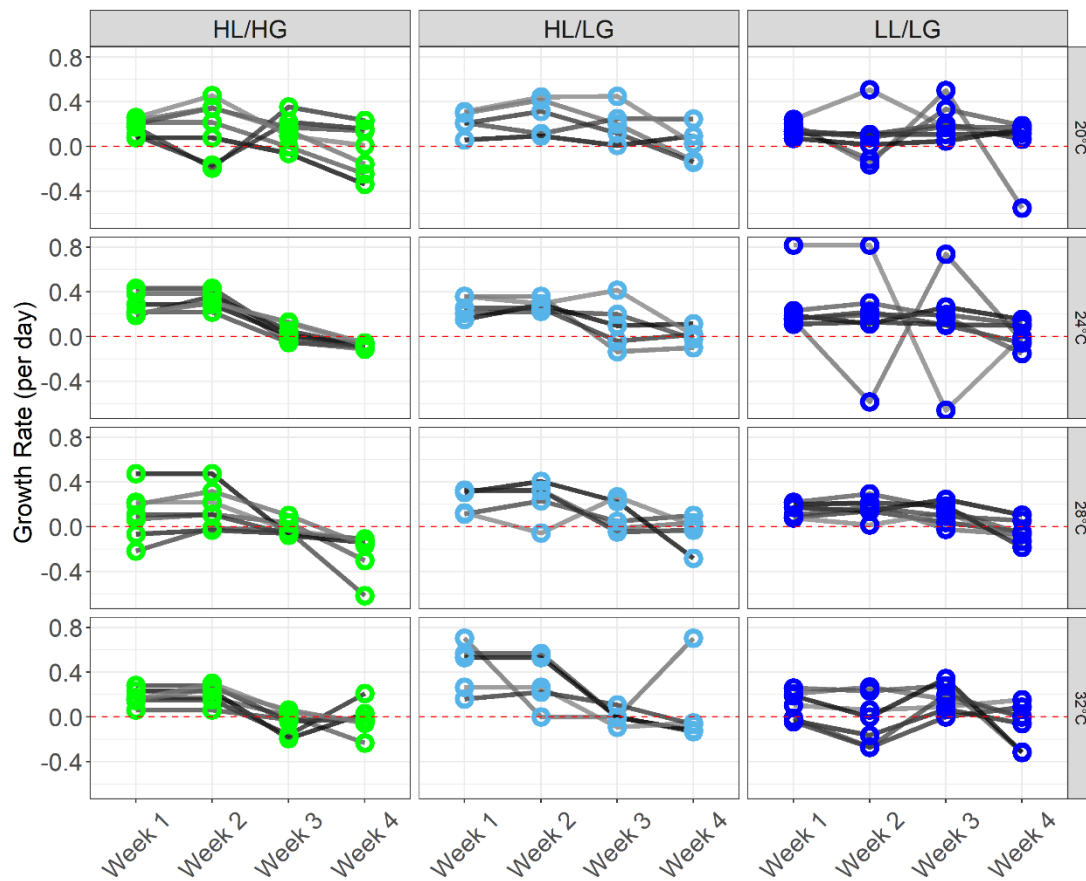


**Figure S3.** Bacterial type significantly predicts the growth rates of *M. aeruginosa*. Alternative illustration of the data represented in Fig 3 and Fig S3. Note that Week 1 and exponential phase are synonymous. LME with week of study (= phase) as a fixed effect: type  $F_{2,16}=6.42$ ,  $p=0.009$ ,  $\eta^2_p=0.45$ ; temperature  $F_{3,267}=2.73$ ,  $p=0.045$ ,  $\eta^2_p=0.03$ ; phase  $F_{3,267}=29.80$ ,  $p<0.0001$ ,  $\eta^2_p=0.25$ ; type\*temperature  $F_{6,267}=1.23$ ,  $p=0.289$ ; type\*phase  $F_{6,267}=3.38$ ,  $p=0.003$ ,  $\eta^2_p=0.07$ . GAM with phase as a fixed factor, best model  $S$ : type-specific trendlines (with no global trendline)  $p=0.004$ ,  $R^2=24.3\%$ .

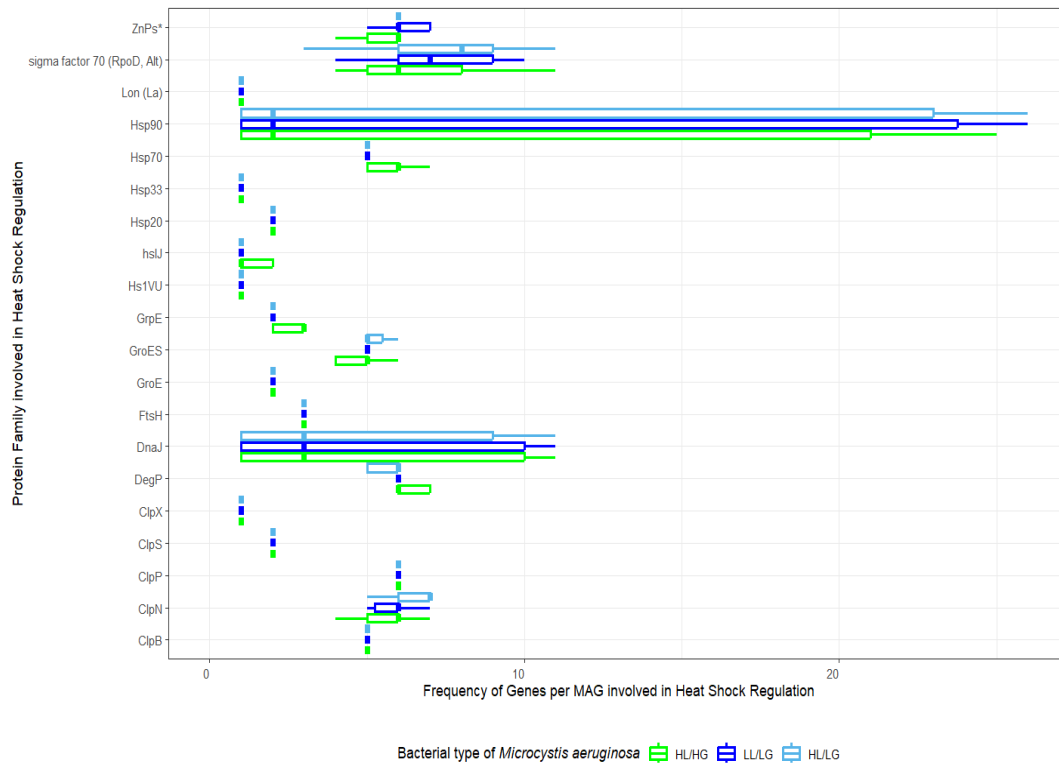


**Fig S4.** In addition to monitoring expression during the warming study, we surveyed the frequency of genes encoding for proteins involved in heat shock regulation among strains of *M. aeruginosa* based on an analysis of metagenome assembled genomes of three bacterial types isolated from inland lakes of Michigan. ZnPs is an abbreviation for Zn-dependent protease with chaperone function. Also note that as this count data was not normally distributed, we used a general linear model with a Poisson distribution, bacterial type as a fixed effect, and gene nested within strain as a random effect. Though some variation in gene number is evident, bacterial type was not a significant predictor of patterns in gene number for either the full model across all genes, or individual models considering each gene individually (all p-values > 0.05).

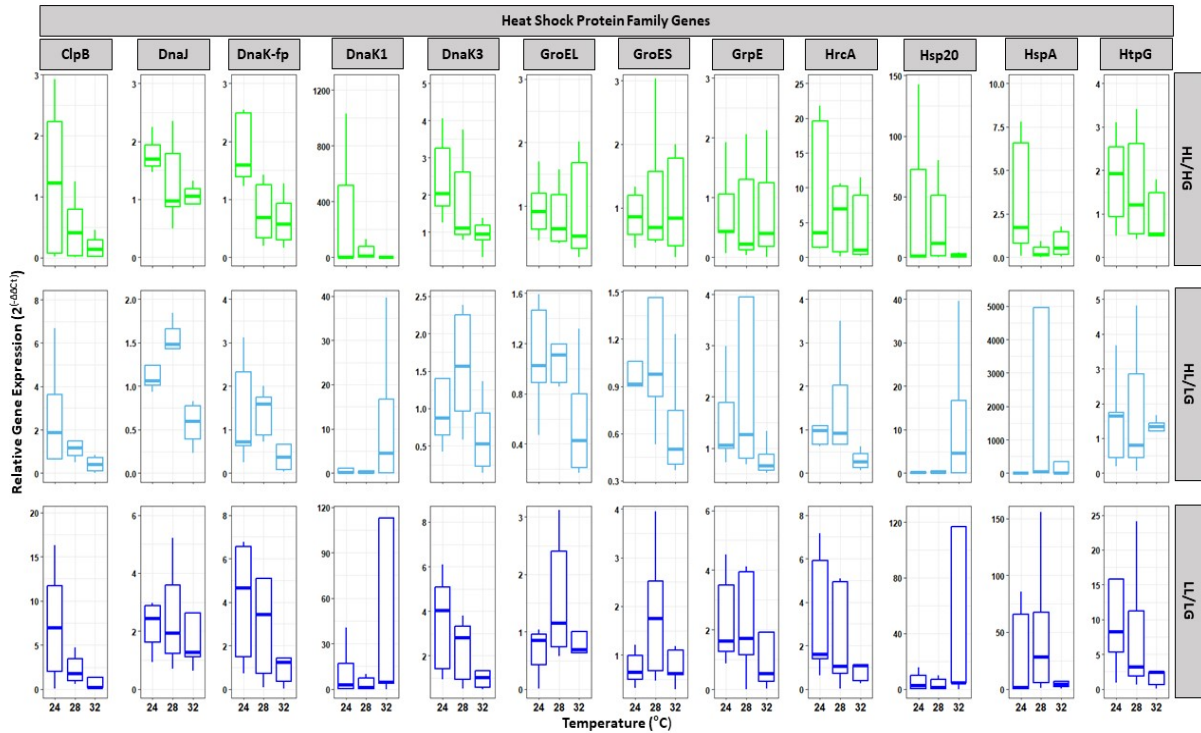


**Fig S5.** Alternative illustration of the data represented in **Fig 4** is shown to emphasize downregulation of most genes encoding for heat shock proteins in *M. aeruginosa* with temperature (ANOVA: temperature -  $F_{2, 402} = 10.02$ ,  $p < 0.01$ ; type -  $F_{2, 16} = 2.17$ ,  $p = 0.12$ ; type x temperature interaction -  $F_{4, 402} = 3.67$ ,  $p < 0.01$ ). Relative gene expression was calculated as  $2^{(-\Delta\Delta Ct)}$ , with *rpoA* as the reference gene and 20°C as the reference condition. To facilitate data visualization, each faceted plot has its own y-axis. Note that such downregulation is expected among constitutively expressed heat shock proteins, however two genes show a clear deviation, sharply increasing with temperature among oligotrophic genotypes, which is indicative of their role as inducible chaperones playing a key role in the heat shock response: DnaK1 and Hsp20. For these two genes, there was a significant type x temperature interaction: DnaK1 ( $F_{4, 28} = 2.83$ ,  $p = 0.044$ ) and Hsp20 ( $F_{4, 28} = 2.90$ ,  $p = 0.040$ ).

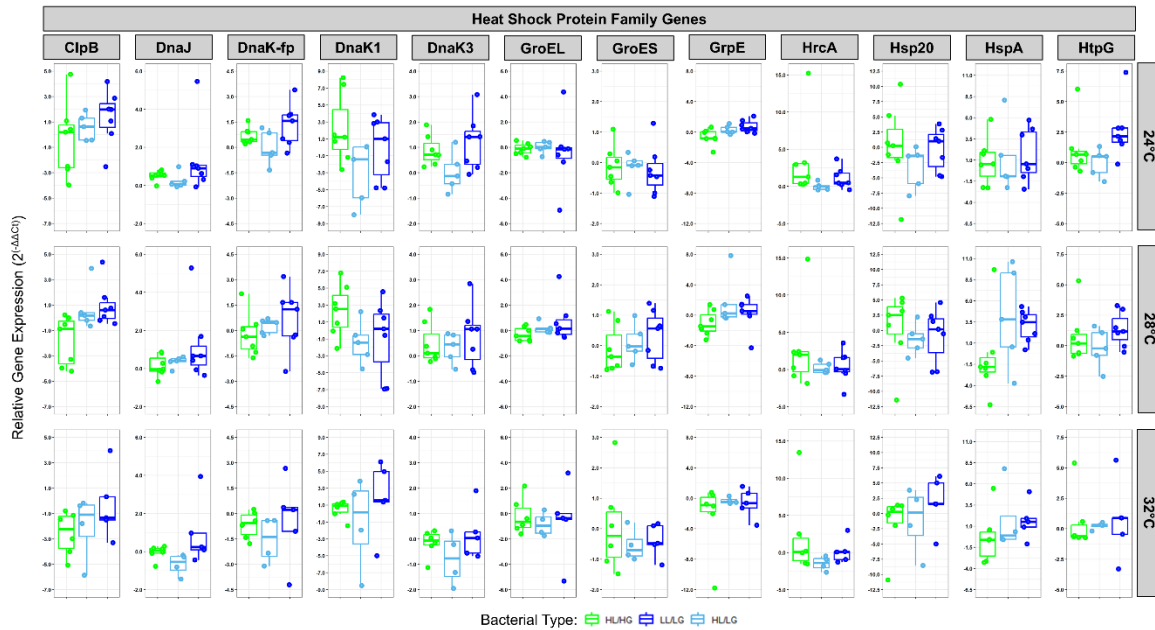


**Figure S6.** Bacterial type-specific responses to temperature of *M. aeruginosa* through the differential expression of genes encoding for heat shock proteins (ANOVA on all HSPs: temperature-  $F_{2, 402} = 10.02$ ,  $p < 0.01$ ; type-  $F_{2, 16} = 2.17$ ,  $p = 0.12$ ; type x temperature interaction -  $F_{4, 402} = 3.67$ ,  $p < 0.01$ ). Type-specific responses to temperature were also observed for two models run on individual gene targets (DnaK1 type x temperature interaction:  $F_{4, 28} = 2.83$ ,  $p = 0.044$ ; Hsp20 type x temperature interaction:  $F_{4, 28} = 2.90$ ,  $p = 0.040$ ). Note that relative gene expression was calculated as  $2^{-\Delta\Delta C_t}$ , with *rpoA* as the reference gene and 20°C as the reference condition and that data were boxcox transformed before statistics. Unlike Fig 4 & S5 the transformed rather than the raw data is plotted here.

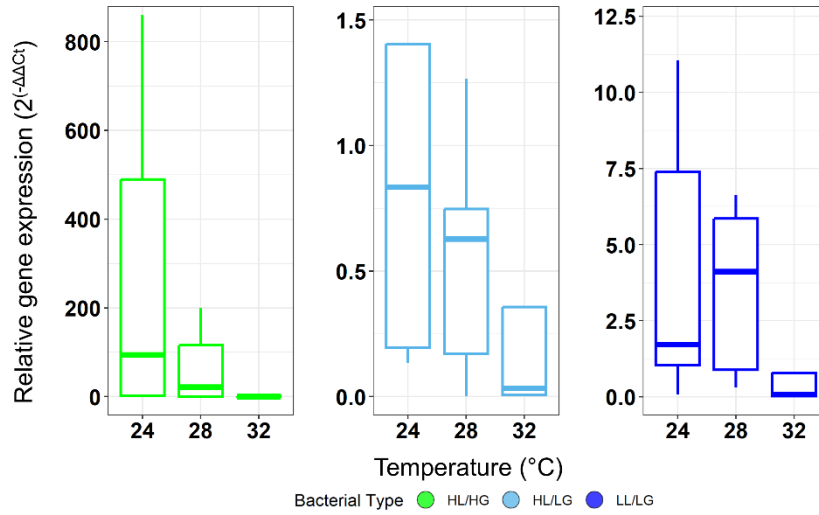


**Fig S7.** Elevated temperatures caused a similar decline in expression of the *mcyE* toxin gene across each of three bacterial types of *M. aeruginosa*. This gene encodes for a protein in the microcystin hepatoxin production pathway. Linear mixed effects model for *mcyE*:  $F_{2,28} = 12.09$ ,  $p < 0.001$ .

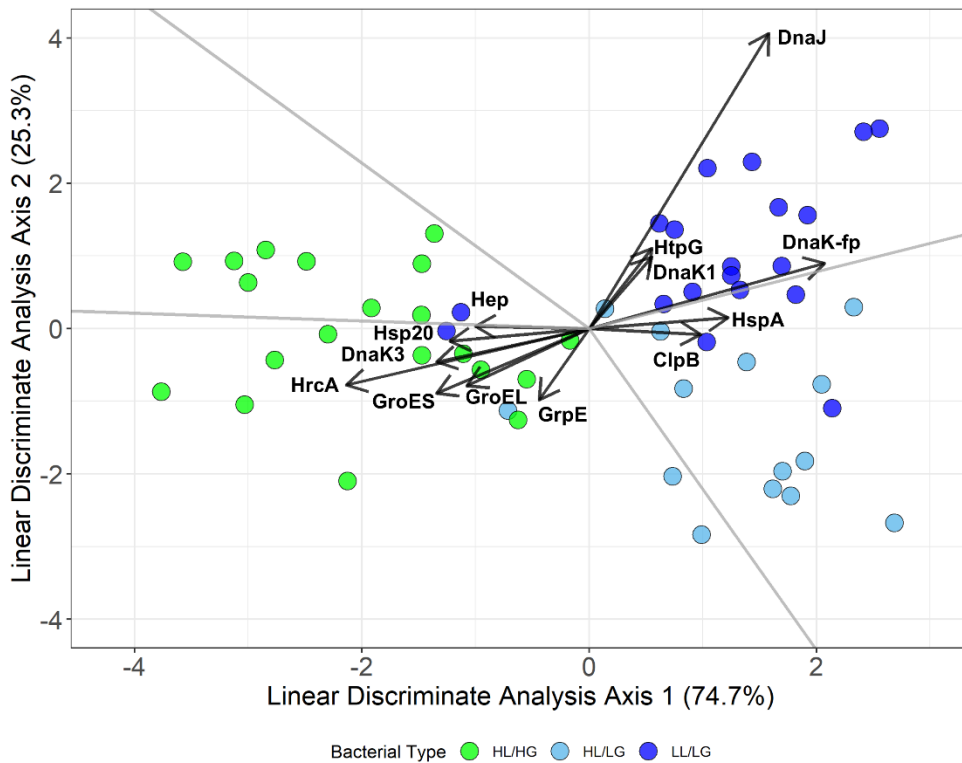


**Figure S8.** Bacterial types show significantly different overall patterns in growth and expression dynamics (MANOVA: type -  $F_{34,58}=3.25$ ,  $p<0.0001$ ,  $\eta^2_p=0.66$ ; temperature -  $F_{34,58}=1.33$ ,  $p=0.167$ ,  $\eta^2_p=0.44$ ; type\*temperature:  $F_{68,124}=0.69$ ,  $p=0.952$ ,  $\eta^2_p=0.28$ ). Distinct clustering of bacterial types is illustrated using a Linear Discriminate Analysis with arrows representing the coefficients of variance explained by each variable in the model. To aid in better visualization of gene expression arrows, relative to Fig 5, the length of all arrows was multiplied by 4. Data for all temperatures except 20°C is included in the analysis to enable the calculation of relative gene expression with 20°C as the baseline.

**Table S3.** Coefficients for discriminant functions illustrated in Fig. 5 & S8. HSP = Heat Shock Protein

<b>Trait</b>	<b>Category</b>	<b>DF1</b>	<b>DF2</b>
ClpB	HSP Expression	0.2452219	-0.020266293
DnaJ	HSP Expression	0.3949882	1.015767325
DnaK-fp	HSP Expression	0.5177078	0.22510684
DnaK1	HSP Expression	0.1376740	0.246831888
DnaK3	HSP Expression	-0.3358387	-0.114430812
GroEL	HSP Expression	-0.2691971	-0.196500875
GroES	HSP Expression	-0.3356082	-0.222568824
GrpE	HSP Expression	-0.11022	-0.24519
Hep	Toxin Production Pathway Expression	-0.24996	0.008437
HrcA	HSP Expression	-0.5341	-0.1945
Hsp20	HSP Expression	-0.30609	-0.04386
HspA	HSP Expression	0.305893	0.036885
HtpG	HSP Expression	0.138031	0.275579
ExpPhase (Week 1)	Growth Dynamics	1.381906	-3.05586
Week 2	Growth Dynamics	-1.05839	1.207324
Week 3	Growth Dynamics	2.806489	1.098374
Week 4	Growth Dynamics	-2.2787878	0.121005699

## Supplementary References

1. Huntemann, M., Ivanova, N. N., Mavromatis, K., Tripp, H. J., Paez-Espino, D., Palaniappan, K., ... Kyrpides, N. C. (2015). The standard operating procedure of the DOE-JGI Microbial Genome Annotation Pipeline (MGAP v.4). *Standards in Genomic Sciences*, 10, 86.
2. Jackrel, S. L., White, J. D., Evans, J. T., Buffin, K., Hayden, K., Sarnelle, O., & Deneff, V. J. (2019). Genome evolution and host-microbiome shifts correspond with intraspecific niche divergence within harmful algal bloom-forming *Microcystis aeruginosa*. *Molecular Ecology*, 28(17), 3994–4011.
3. Janse I, Meima M, Kardinaal WEA, Zwart G. 2003 High-resolution differentiation of cyanobacteria by using rRNA-internal transcribed spacer denaturing gradient gel electrophoresis. *Appl. Environ. Microbiol.* **69**, 6634–6643.
4. Dick GJ, Duhaime MB, Evans JT, Errera RM, Godwin CM, Kharbush JJ, Nitschky HS, Powers MA, Vanderploeg HA, Schmidt KC, Smith DJ, Yancey CE, Zwiers CC, Deneff VJ. 2021 The genetic and ecophysiological diversity of *Microcystis*. *Environ. Microbiol.* **23**, 7278–7313.
5. Kashtan N *et al.* 2014 Single-Cell Genomics Reveals Hundreds of Coexisting Subpopulations in Wild Prochlorococcus. *Science* **344**, 416–420.
6. Kettler GC *et al.* 2007 Patterns and Implications of Gene Gain and Loss in the Evolution of Prochlorococcus. *PLoS Genetics* **3**, e231.
7. Yu G, Smith DK, Zhu H, Guan Y, Lam TTY. 2017 ggtree: an r package for visualization and annotation of phylogenetic trees with their covariates and other associated data. *Methods Ecol. Evol.* **8**, 28–36.
8. Wetzel, R. G. *Limnology: Lake and River Ecosystems*. (Gulf Professional Publishing, 2001).
9. Raikow DF, Sarnelle O, Wilson AE, Hamilton SK. 2004 Dominance of the noxious cyanobacterium *Microcystis aeruginosa* in low-nutrient lakes is associated with exotic zebra mussels. *Limnology and Oceanography* **49**, 482–487.
10. Sarnelle O, Wilson AE, Hamilton SK, Knoll LB, Raikow DF. 2005 Complex interactions between the zebra mussel, *Dreissena polymorpha*, and the harmful phytoplankter, *Microcystis aeruginosa*. *Limnology and Oceanography* **50**, 896–904.
11. Livak KJ, Schmittgen TD. 2001 Analysis of relative gene expression data using real-time quantitative PCR and the 2- $\Delta\Delta$ CT method. *Methods* **25**, 402–408.
12. Pedersen EJ, Miller DL, Simpson GL, Ross N. 2019 Hierarchical generalized additive models in ecology: an introduction with mgcv. *PeerJ* **7**, e6876.
13. Wood, S. N. (2017). *Generalized additive models: An introduction with R* (2nd ed.). Chapman and Hall/CRC.
14. Venables WN, Ripley BD. 2002 *Modern Applied Statistics with S*, 4th ed. 4th edn. New York, NY: Springer.
15. R Core Team. 2023 R: A language and environment for statistical computing.
16. Pinheiro J, Bates D, DebRoy S, Sarkar D, Heisterkamp S, Willigen BV, Ranke J, R Core Team. 2023 nlme: linear and nonlinear mixed effects models.
17. Pinheiro J, Bates D. 2000 *Mixed-Effects Models in S and S-PLUS*. New York: Springer-Verlag.
18. Christensen RHB. 2023 ordinal---regression models for ordinal data.
19. Lenth RV *et al.* 2024 emmeans: Estimated Marginal Means, aka Least-Squares Means.
20. Borcard D, Gillet F, Legendre P. 2011 *Numerical Ecology with R*. New York, NY: Springer.
21. Wickham H. 2016 *ggplot2*. Cham: Springer International Publishing.

22. QGIS Development Team (2024). QGIS Geographic Information System. Open Source Geospatial Foundation Project.